REPORT

Åknes rock slope

MONITORING OF DISPLACEMENTS

DOC.NO. 20180662-05-R
REV.NO. 0 / 2020-07-09

NORWEGIAN GEOTECHNICAL INSTITUTE
NGI.NO

Project

Project title:	Drainage Åknes
Document title:	Monitoring of displacements in the Åknes rock slope
Document no.:	20180662-05-R
Date:	2020-07-09
Revision no. /rev. date:	0 /

Client

Client:	NVE
Client contact person:	Gustav Pless
Contract reference:	Research and development contract, signed 12 September 2018

for NGI

Project manager:	Kristin H. Holmøy
Prepared by:	Mahdi Shabanimashcool, Henrik Langeland, Kristin H. Holmøy
Reviewed by:	Vidar Kveldsvik

NORWEGIAN GEOTECHNICAL INSTITUTE
NGI.NO

Main office
PO Box 3930 Ullevaal St.
NO-0806 Oslo
Norway

Trondheim office
PO Box 5687 Torgarden
NO-7485 Trondheim
Norway

T 22 02 30 00
F 22 23 04 48
NGI@ngi.no

BIC NO. DNBANOKK
IBAN NO26 5096 05 01281
ORGANISATION NO.
958 254 318MVA

ISO 9001/14001
CERTIFIED BY BSI
FS 32989/EMS 612006

Contents

Appendix

Review and reference page

1 Introduction

This report summarizes the results of NGI's activities on processing and analysing monitoring data from Åknes. The analysis is limited to a number of devices and does not cover the entire dataset available (with regard to time and devices) from Åknes. However, the presented approach may be used to further assess the data from Åknes monitoring system.

The aim of the analysis is to study the movement nature of the Åknes rock-slope and updated existing geological information. The study also is helpful to select and generate geological cross-sections for the numerical modelling. In addition, it was intended to see if there are any correlations between the groundwater changes and displacements at the study site or not.

All data used in the analysis is provided by NVE. This report does not describe technical specifications related to measurement instrumentation.

The following instrumentations at Åknes have been analysed, with the locations shown in the map (Figure 1);

1. GPS (red marking)
2. DMS instrumented in boreholes (purple marking)

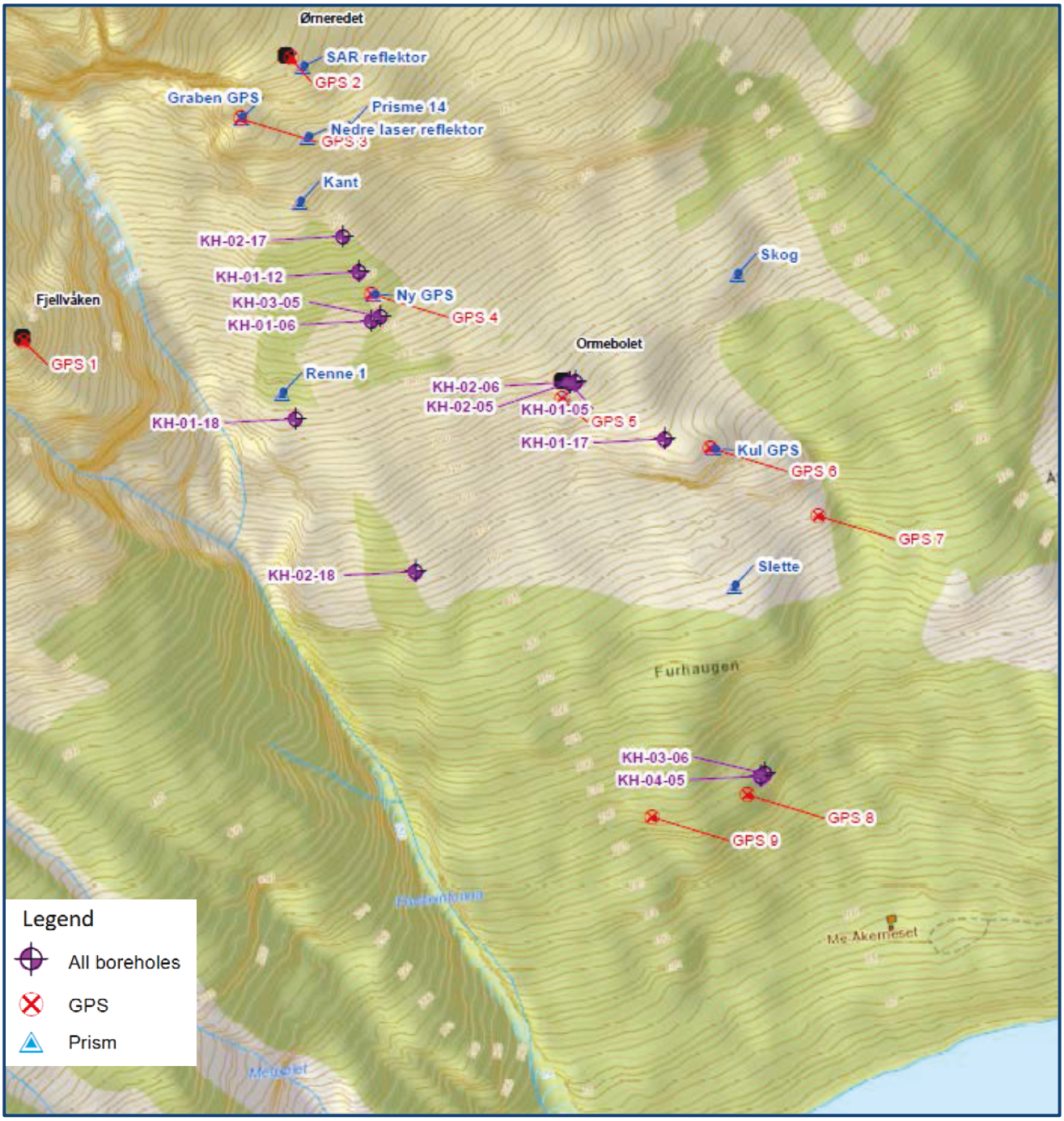

Figure 1. Location of the studied instruments.

2 Data analysis

The field measurements data are in the format of "displacement – time" series; and they were used to obtain velocity and acceleration of the Åknes rock slope. Several MATLAB scripts were developed to process the data and obtain the velocity and acceleration of the sliding mass.

For the field measurements the following Cartesian coordinate was assumed:

- Vertical direction is assumed as Z-axis. Upward is positive and downward is negative values.
- Horizontal in East-West direction as X-axis. Toward East is positive and toward West is negative.
- Horizontal in North-South direction as Y-axis. Toward North is positive and toward South is negative.

The displacement vectors at the time of t_i can be expressed as (Note that all the **bold values** in this report are vectorized values):

$$\boldsymbol{X}(\boldsymbol{t_i}) = x(t_i)\boldsymbol{i} + y(t_i)\boldsymbol{j} + z(t_i)\boldsymbol{k} \quad (1)$$

The velocity can be obtained for the time t_i:

$$\boldsymbol{V}(\boldsymbol{i}) = v_x\boldsymbol{i} + v_y\boldsymbol{j} + v_z\boldsymbol{k} \quad (2)$$

Where
$v_x = \frac{x(t_{i+1})-x(t_i)}{t_{i+1}-t_i}$, $v_y = \frac{y(t_{i+1})-y(t_i)}{t_{i+1}-t_i}$ and $v_z = \frac{z(t_{i+1})-z(t_i)}{t_{i+1}-t_i}$

The acceleration at the time of t_i is also defined as

$$\boldsymbol{a} = a_x\boldsymbol{i} + a_y\boldsymbol{j} + a_z\boldsymbol{k} \quad (3)$$

Where
$a_x = \frac{v_x(t_{i+1})-v_x(t_i)}{t(i+1)-t(i)}$, $a_y = \frac{v_y(t_{i+1})-v_y(t_i)}{t(i+1)-t(i)}$ and $a_z = \frac{v_z(t_{i+1})-v_z(t_i)}{t(i+1)-t(i)}$

The dip angle of the displacements / velocity /accelerations was calculated as:

$$dip = \tan^{-1}\left(\frac{\Delta Z}{\sqrt{\Delta X^2+\Delta Y^2}}\right) \quad (4)$$

Where ΔX, ΔY and ΔZ is the displacement in a specific period, for example:
$\Delta X = x(t_{i+1}) - x(t_i)$

ΔX, ΔY and ΔZ can be changed to corresponding values in velocity and acceleration as well as dip angle of velocity and acceleration.

Dip-direction (DD) of the displacement / velocity / acceleration is calculated with the following technique. First, the X-Y plane is divided to four sections (Figure 2) and then the calculations were carried out as presented in Table 1.

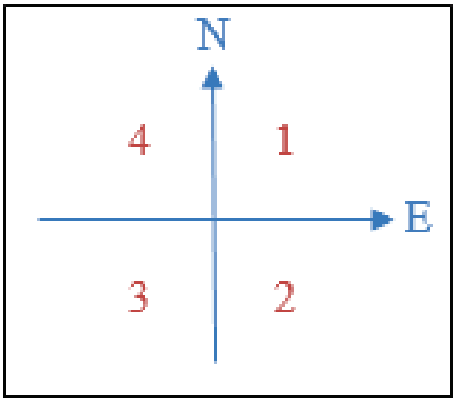

Figure 2. The horizontal plane (X-Y plane) is divided in 4 zones to calculate the dip/ dip-direction of the displacement / velocity / acceleration (see Table 1 for the calculations).

Table 1. Calculating dip-direction of the movements. The zoning is defined in Figure 2.

Zone	Axiom	Calculation of dip direction
Zone 1	If ΔX & $\Delta Y \geq 0$	$DD = \tan^{-1}\left(\frac{\Delta X}{\Delta Y}\right)$
Zone 2	If $\Delta Y \leq 0$ & $\Delta X \geq 0$	$DD = 90° + (90° - \tan^{-1}\left(\frac{\Delta X}{\lvert\Delta Y\rvert}\right)$
Zone 3	If $\Delta Y \leq 0$ & $\Delta X \leq 0$	$DD = 180° + \tan^{-1}\left(\frac{\lvert\Delta X\rvert}{\lvert\Delta Y\rvert}\right)$
Zone 4	If $\Delta Y \geq 0$ & $\Delta X \leq 0$	$DD = 360° - \tan^{-1}\left(\frac{\lvert\Delta X\rvert}{\Delta Y}\right)$

From the physics point of view (static) if a body is in equilibrium the acceleration ($\boldsymbol{a}$) is zero:

$$\sum \boldsymbol{F} = m\boldsymbol{a} = 0 \qquad (5)$$

where $\boldsymbol{F}$ is the force; and m the mass of the body. However, $\boldsymbol{a}=0$ does not mean that the displacement and velocity are equal to zero. It means that the velocity is either a constant value or zero.

When velocity starts to change with time, then acceleration is $\boldsymbol{a} \neq 0$; meaning that $\sum \mathbf{F} \neq 0$. Hence, at that the time there are external effects (for example, groundwater, earthquake, reduced shear strength etc.) which is changing the force equilibrium condition of the moving body.

To understand the failure mechanism of the slope, we must look at the slope movement process and how it changes over time. Figure 3 shows three different scenarios of displacement which might be relevant for a slope (Wyllie & Mah, 2004) [1]:

- Regressive: cycles of accelerations if external force is imposed. As soon as the external force is gone, the moving mass goes toward stabilising. The external force can for example be groundwater rise / increased water head. In this case the frictional resistance of the sliding

surface is enough to stabilise the slope if the external disturbance is remove or sufficiently reduced.

- Progressive: in this behaviour gradual increase in slope velocity can be observed. The frictional resistance of the sliding surface is not enough to stabilise the slope and it is unstable.
- Progressive – regressive behaviour can be observed if intact rock fracturing is happening and a sliding plane is developing inside the rock mass (the sliding plane has not been fully developed yet). With considering the fracture mechanics of the rocks under sub-critical conditions, it is possible to describe progressive – regressive behaviour more in detail (Jaeger et al. (2007), Atkinson (1987) and Sullivan (2007)) [2, 3 and 4]. In the progressive – regressive behaviour, the acceleration is not due to the external forces and it happens naturally in the rock mass due to fracture propagations inside the intact rock materials. It can be related to some environmental factors if fracturing happens in sub-critical level. For example, large changes in the temperature and water content of the rock can decrease the fracture toughness and allow further propagation of the fracture.

Identifying the progressive and regressive behaviour of the slopes is a key factor in slope monitoring. The velocity changes dependent on the geology and nature of the slide. However, gathered data from open pit mines showed wide variation of critical velocities short time before failure (Sullivan (2007) [4]. Ryan and Call [5] suggested that a critical velocity, when failure could be expected in short time is ca. 12 mm/day.

In addition, further investigations are required to find how the displacement in the different parts of the slope are correlating with each other. The Åknes rock slope is studied over decades, and as described in Kveldsvik [6] the rock slope may be divided in 12 blocks which have different behaviour and movement patterns.

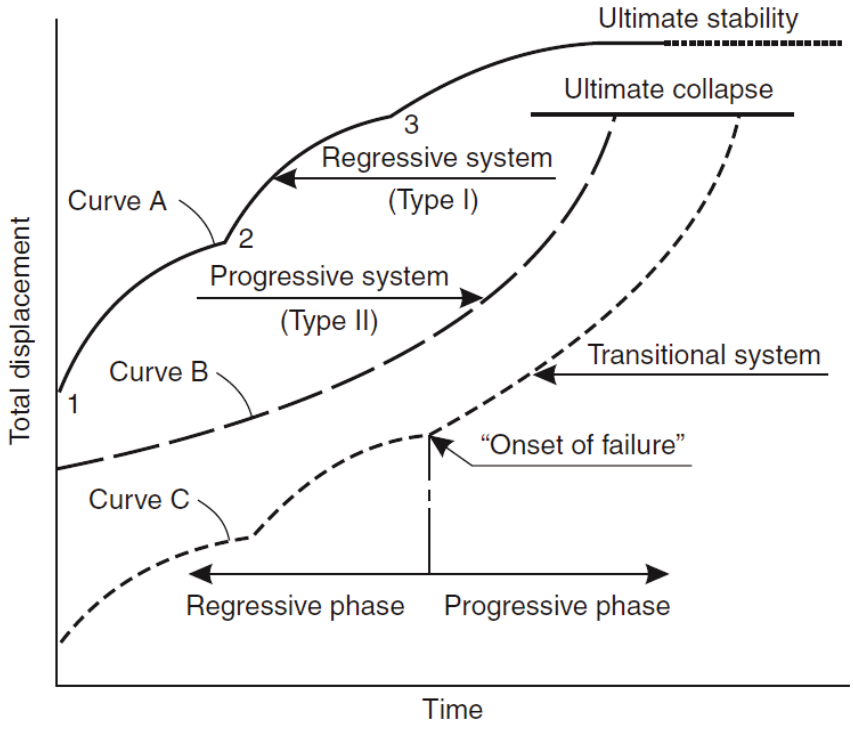

Figure 3. Interpreting observed displacements in the rock-slopes, from Wyllie & Mah (2004) [2]

3 GPS

Table 2 presents a list of active GPS devices in Åknes. They have been active for seven years. Appendix A shows the velocity and accelerations calculated for data from GPS-displacement – time series obtained from the GPS monitoring data.

Table 2. GPS monitoring time for data extraction.

GPS	Start Date/time	Stop Date/time	Months and days
2	13.10.2011 /12:00	17.10.2018 /18:00	84 mos., 5 d.
3	13.10.2011 /12:00	17.10.2018 /18:00	84 mos., 5 d.
4	13.10.2011 /12:00	23.09.2018 /18:00	83 mos., 11 d.
5	13.10.2011 /12:00	17.10.2018 /18:00	84 mos., 5 d.
6	13.10.2011 /12:00	17.10.2018 /18:00	84 mos., 5 d.
7	14.10.2011 /12:00	17.10.2018 /18:00	84 mos., 4 d.
8	13.10.2011 /12:00	17.10.2018 /18:00	84 mos., 5 d.
9	13.10.2011 /12:00	17.10.2018 /18:00	84 mos., 5 d.

4 DMS

4.1 Measurements

The biggest advantage of the DMS-sensors installed in boreholes, versus regular inclinometers, is that it is possible to have an early warning system based on the sub-surface displacements, rather than just surface instrumentation. However, it has a disadvantage over the classical inclinometers, since the DMS-sensors are connected to the rock mass by a small plastic spacer. In some places, by the time the spacers can slide or deform, leading to faulty results. Hence, in our analysis, we checked the local cumulative displacement at specific depth versus time, to check whether there was error in the data. Table 3 shows available DMS data at the site and the period instrumentation was active. The data from DMS are horizontal displacement in North and East directions versus time (see Chapter 2).

The data from inclinometers shows the relative shape of the inclinometer casing to the initial condition. Plotting the magnitude of change at each reading depth is useful to identify potential zones / planes of movement. The most common type of graph displays cumulative lateral deformation with depth, starting at the bottom of the casing as zero and summarizing increments of displacement for each measured interval up to the ground surface. Change in the cumulative displacement graph, if it happens on a specific depth, show a potential sliding plane or a sliding zone. Plots can be developed to illustrate the location of deformation zones clearly.

Table 3. Available DMS monitoring time at data extraction.

Total station	Start Date/time	Stop Date/time	Months and days
KH-01-06	22.11.2010	15.07.2013	31 mos., 23 d.
KH-02-06	21.09.2015	21.10.2019	49 mos.

Total station	Start Date/time	Stop Date/time	Months and days
KH-03-06	21.09.2015	21.10.2019	49 mos.
KH-01-12	24.09.2015	24.09.2019	48 mos.
KH-01-17	15.10.2018	14.01.2019	3 mos.
KH-02-17	15.10.2018	21.08.2019	10 mos., 6 d.

4.2 Potential errors

Graphs of cumulative displacement versus depth can be affected by systematic errors. Systematic errors are mostly handled by monitoring software and we are not going to discuss them further. However, there are some errors that could happen because of detaching of the DMS sensors from the rock mass. Then the shape of cumulative displacement could become as presented in Figure 4. For classical inclinometers, this error is called rotational error. By detaching the inclinometer casing from the rock mass, the inclinometer casing experiences excessive rotational deformation. In rotational error, the measurements in one of the directions (axis A) can also capture deflection in another axis direction (axis B). This type of error can happen in DMS if they detach and start to deform under their own weight. For handling such error, the cumulative displacement at some selected depth versus time was checked (for example plot displacement for every 5 m along the hole) leading to identifying location of a potential sliding plane or zones. Since displacement in A-direction shows a portion of the movement in B-direction, it is possible to correct the measurements in A-direction by deducting measured displacement in B-direction from it (Figure 4) Green & Mikkelsen [7].

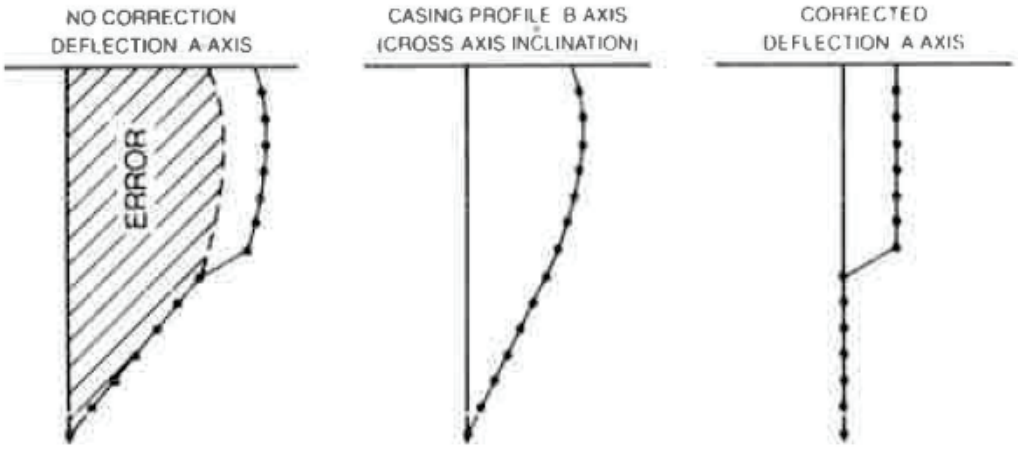

Figure 4. Correcting the measurements when the sensors are detached and rotated inside the borehole [7].

5 Identify sliding planes or zones from DMS data

DMS data show several locations in each borehole with possibility of being identified as sliding planes/zones. However, these depths must be checked against the available core pictures or logs to be verified; unless they are possibly just errors in the DMS. Table 4 summarizes depths where there are large changes (or jumps) in the displacements measured by DMS and whether they are sliding plane or

not. Note that between the available boreholes, KH-01-2006 was ignored since it was not possible to correlate it with the available core logs.

Appendix B shows correlation between the cores (pictures or core logs) and the marked sliding planes in the boreholes from the DMS data.

Table 4. Locations with visible jump / stepping in displacements measured by DMS and verifying them against core pictures whether they are sliding plane / zone.

Borehole	Depths with sharp changes in the displacement / depth curves	Comment	Sliding plane/zone?
KH-02-2006	34 m	There is evidence of sliding plane in core logs.	Yes
	115 m	No evidence of sliding plane in core logs.	No
KH-03-2006	No sharp changes, only small steps in upper part of borehole	No core picture available. Based on core logs it is confirmed that there is no sliding plane in this depth.	No
KH-01-2012	31 m	Confirmed by cores	Yes
	63 m	Confirmed by cores	Yes
KH-01-2017	35 m	Data from core does not show any sliding plane.	No
	40 - 41 m	Confirmed by core; 5 to 10 cm of sliding plane	Yes
KH-02-2017	33 m	Confirmed by cores, 2-3 m of sliding zone	Yes
	71 m	Confirmed by cores, 10 cm of sliding zone	Yes
KH-01-2018	35.5 m	Confirmed by core picture	Yes
	94.5	There is no sliding plane visible in cores	No
KH-02-2018	15 m	Confirmed by core picture	Yes
	112 m	There is no sliding plane visible in cores	No

DMS in boreholes KH-03-2006 and KH-01-2012 show rotational errors, as shown in Figure 4. Therefore, the corrected version of the data is used to obtain the locations with large deviation in the displacements. In these boreholes the corrected displacement in the north direction is calculated by deducting the measured displacement in the East direction from the measured displacements in the north direction. In addition to confirming the location of the sliding plane by the core pictures / logs, they were controlled by checking the cumulative displacement versus time of some specific depth above and under the identified sliding planes.

6 Interpretation of the monitoring results

6.1 Sub-surface and surface displacements (DMS and GPS)

Table 5 and Table 6 present mean velocity and its azimuth measured on the ground surface by GPS and in subsurface by DMS data, respectively.

From Table 5 and Table 6, there are two dominating displacement directions with azimuth of 185 – 225 and 135-143 degrees in the West and East flank, respectively. The slope can, therefore, be divided into two different sections denoted as West and East flank. This is also reported in earlier analyses on the deformations at Åknes and it has been correlated with the folding of the foliation at the site NGU (2007) [8]. Hence, the West and East sections of the slope is denoted as West and East flank, respectively.

Moreover, folding and different angle of the foliation may be the reason that the West and East flanks have also different mean sliding velocity, confirming two separate sliding environments. In addition, in the West flank DMS in the uppermost boreholes (KH-02-2012 and KH-02-2017) show evidence of two sliding planes (denoted as S1 and S2) while in the East flank just one sliding plane is discovered (S3).

Table 5. Mean sliding velocity and directions from DMS on different sliding planes/zones.

Borehole	Depths of sliding plane (m)	Belong to west (W) or east (E) flank	Azimuth of disp. (degree)	Sliding plane name	Mean horizontal sliding velocity (mm/day)
Kh-02-2006	36 m	E	Not possible to measure.	S3	
KH-03-2006	No sliding plane	-	-	No sliding plane	0
KH-01-2012	31 m	W	220 - 224	S2	Not possible to assess velocity due to error in DMS readings
	63 m	W	224	S1	
Kh-01-2017	40 - 41 m	E	165	S3	0.06
Kh-02-2017	33 m	W	185 - 200	S2	0.21
	71 m	W	188 - 200	S1	0.18
Kh-01-2018	35.5 m	W	201 - 211	S1	0.2
Kh-02-2018	15 m	W	218 - 244	S1	0.2

Table 6. Mean velocity and direction of slope surface movements measured by GPS in East and West flank of the slope.

Sensor	North (mm/day)	East (mm/day)	Vertical (mm/day)	Total (mm/day)	Horizontal (mm/day)	Azimuth of displacement (degree from north)
West Flank						
GPS-3	-0.19	-0.05	-0.28	0.08	0.08	195
GPS-4	-0.32	-0.06	-0.36	0.14	0.13	190
East Flank						
GPS-5	-0.04	0.03	0.03	0.06	0.05	143
GPS-6	-0.04	0.04	0.04	0.07	0.05	135
GPS-7	-0.08	0.08	0.04	0.12	0.11	135
Toe area						
GPS-8	0	0	0	0	0	0
GPS 9	0	0	0	0	0	0

Measurements in KH-03-2006 and GPS 8 and 9 show that there is no displacement in the lower section of the slope, denoted as toe area initially by Ganerød (2008) and Jaboyedoff (2011) [9 and 10]. However, some uplift and contraction in vertical direction are discovered. This is interpreted to be correlating with the rock surface temperature changes during summer and winter, and not actually movements/uplift caused by sliding.

Measured sliding direction and orientations are slightly different from GPS and DMS data. However, comparing the data from DMS which has not been subjected to the rotational error, shows that there are good correlations between DMS and GPS in terms of mean velocity direction (or mean displacement direction). In terms of magnitude of the displacements, we can compare only horizontal velocities from GPS with DMS data, which show good correlations.

6.2 Analysis of surface displacements in the north-western area

A closer analysis has been done on the north-western area of the Åknes rock slope. Kveldsvik et al. (2008) divided the rock slope in 12 blocks studying displacements on the surface based on photogrammetry in different time frames (1961-1983 and 1983-2004), see Figure 5. In addition, newer displacement measurements from prisms and total stations were used in between 2004 and 2008.

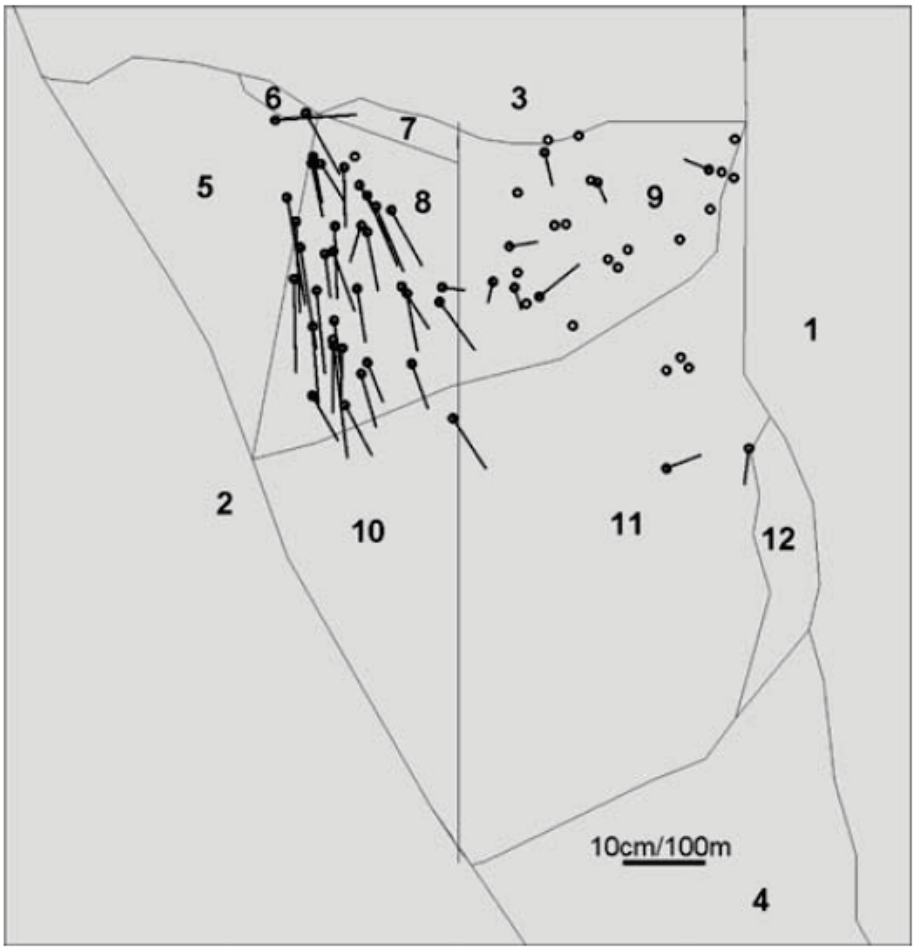

Figure 5. Initial block model and annual average slope displacements derived from photogrammetry 1983-2004. Scale; cm for displacements and m for block model, from Kveldsvik et al. (2008).

Block 8 is an interesting area with registrations of displacements. Therefore, block 8 is chosen for further analysis. Kveldsvik et al. (2008) found that mean horizontal displacements in block 8 was as follows:

- 12,6 cm/year in the period between 1961-1983 (8 points, photogrammetry)
- 7,7 cm/year in the period between 1983-2004 (35 points, photogrammetry)
- 6,8 cm/year in the period between 2004-2006 (total station/prisms)

Today GPS3, GPS4 and NewGPS are active or have been active from 2011/2012. GPS4 is in the central part of block 8, see Figure 6. Registered horizontal displacement from 13th October 2011 to 23rd September 2018 was 4,7 cm/year with azimuth N170E (almost directly South). Furthermore, NewGPS is positioned at the same place as GPS4 (see Figure 6). Registered horizontal displacement for NewGPS in the period 24th June 2012 to 23rd June 2020 was 5,1 cm/year with azimuth N163E. The direction of movement is approximately the same for GPS4 and NewGPS but the displacement is less. Based on the registered displacements in GPS4 and NEWGPS the tendency is that the displacements in block 8 is decreasing with time.

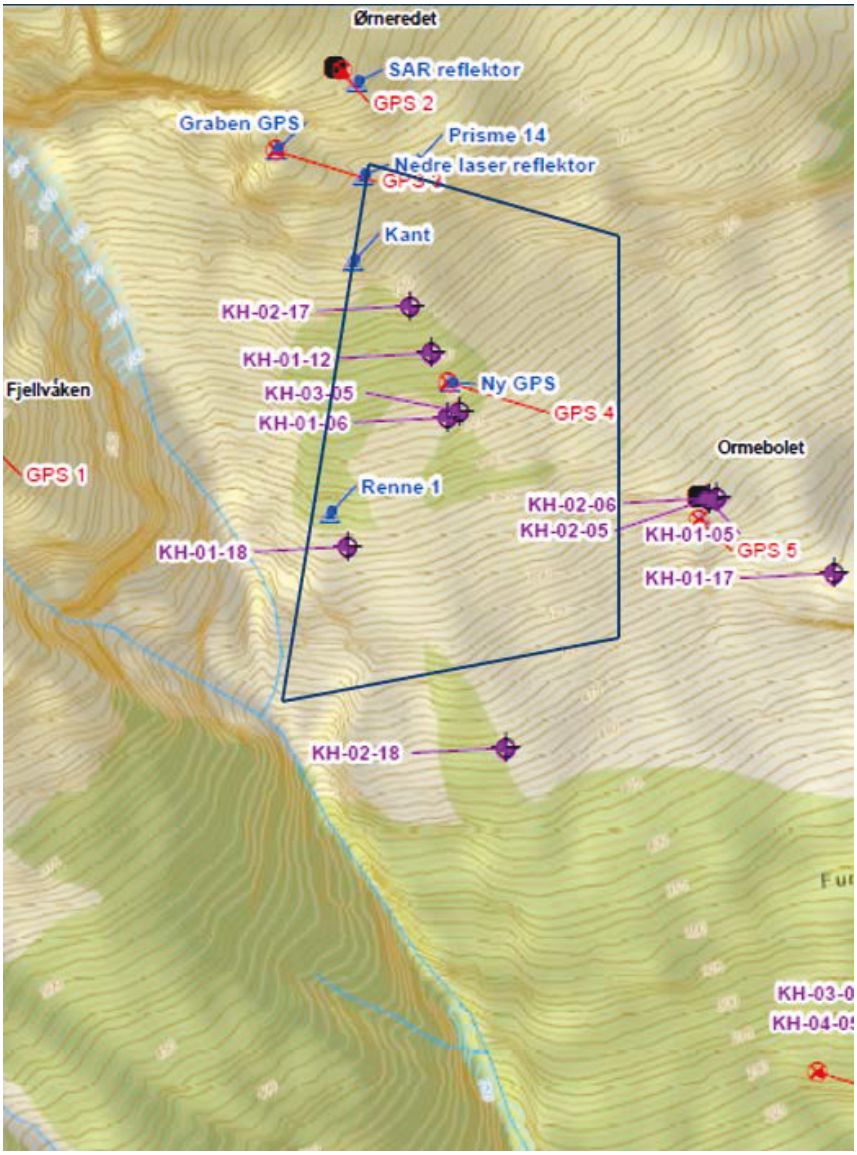

Figure 6 Snip from Figure 1 illustrating approximately location of block 8 (marked with dark blue lines) together with the new boreholes.

6.3 Effect of groundwater on slope movement

Several analyses are carried out to find if there is a correlation between groundwater fluctuations and possible acceleration in the Åknes rock slide. In addition to four sectioned boreholes from 2017 and 2018, monitoring of water table in open boreholes have been done since 2005/2006. An overview of the monitored boreholes is given in Table 7. DMS data is available in the same boreholes plus surface displacements from GPS and prisms can help to decrease uncertainties in the assessments.

Table 7. Overview of boreholes and water table monitoring.

Borehole	Installation	Calibration	Stopped	
KH-01-05	2007	NA	2017	Open
KH-02-05	No monitoring			
KH-03-05	No monitoring			
KH-04-05	2009	NA	2017	Open
KH-01-06	2007	NA	2013	Open
KH-02-06	22-05-2014	20-09-2015	Active	Open
KH-03-06	04-08-2015	18-09-2015	Active	Open
KH-01-12	22-05-2014	24-09-2015	Active	Open
KH-01-17	25-06-2019	06-11-2019	Active	Packers
KH-02-17	29-09-2018	15-10-2018	Active	Packers
KH-01-18	30-10-2019	08-11-2019	Active	Packers
KH-02-18	29-10-2019	08-11-2019	Active	Packers

As we can see from Appendix A and C, the velocity is almost constant. It is possible to fit a linear function to the monitored displacement data from GPS with least square coefficient factor above 98%. No significant acceleration has been observed during the monitoring period.

In the hydrogeological report [11] it was found seasonal variations in the open boreholes with characteristic groundwater level decline during winter and recovery from March/April when the snow melting is high. In the sectioned boreholes (with packers) small seasonal dependency can be seen in the middle part of the boreholes, and the results are changing slowly. No direct correlation with precipitation can be seen. The influence of water infiltration from surface seems to be low since the water table show only small seasonal variation.

When looking at stability assessment, the groundwater pressure at and directly above the sliding plane is the most important parameter reducing the normal stress and the stability. Therefore, the water pressure on or directly above the major identified sliding plane was studied. In the West flank it was found that the water pressure over the monitoring period varied from 0 to 3,5 m, see Table 8 for details. In half of the boreholes the water head is below the sliding plane. The investigation of the slope behaviour versus groundwater should be concentrated on changes of the water head measured on the sliding plane. Unfortunately, available data from KH-01-2018 is limited to winter 2019 and spring 2020. The data period for KH-01-2012 is longer: 24.09.2015-24.09.2019 (Table 3).

Table 8. Overview of registered variation of water pressure on main sliding plane (or close to main sliding plane).

Borehole number	No. of piezo-meters	Water table* (mbgl)	Depth to main sliding plane (mbgl)	Water pressure on main sliding plane (m)
BH-01-06	1	55-60	49-50	0
BH-02-06	1	43,7-45,7	33	0
BH-03-06	1	41,5-44	24	0

Borehole number	No. of piezo-meters	Water table* (mbgl)	Depth to main sliding plane (mbgl)	Water pressure on main sliding plane (m)
BH-01-12	1	~62	62	0-2,7
BH-01-17	9	~35,3	35,5	0-0,5
BH-02-17	11	~66,5	70	2,3-3,5
BH-01-18	10	~33,4	34	0,4-1,4
BH-02-18	12	~18	15	0

*Water table close to the main sliding plane.

Figure 7 shows groundwater table in Borehole KH-01-2012 versus time. Three dates with highest water head was marked to assess whether there are any correlations between the groundwater table and sliding at West flank. As it is visible, the recorded highest water head is always from start of October to middle of November.

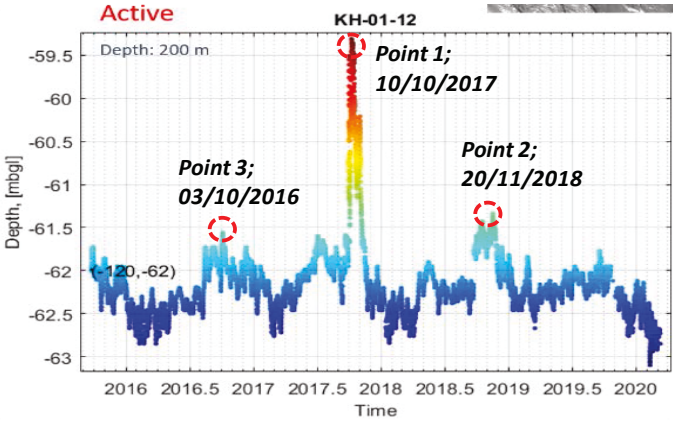

App. water-table: ~62 m

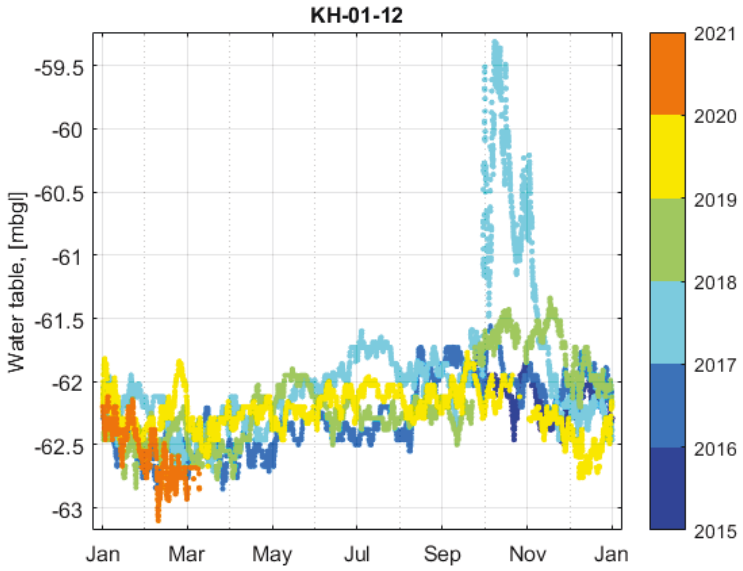

Figure 7. Upper: Recorded groundwater table in open borehole of KH-01-2012 and marked 3 highest recorded water heads. Lower: Groundwater fluctuation in a period of one year for borehole KH-01-2012.

The displacements measured by GPS 3 and 4 which are located in the West flank, are shown as example to investigate the correlation between groundwater changes versus displacements (Figures 8 – 10). They show that there are no visible changes in the displacement rate during those dates with highest marked groundwater level.

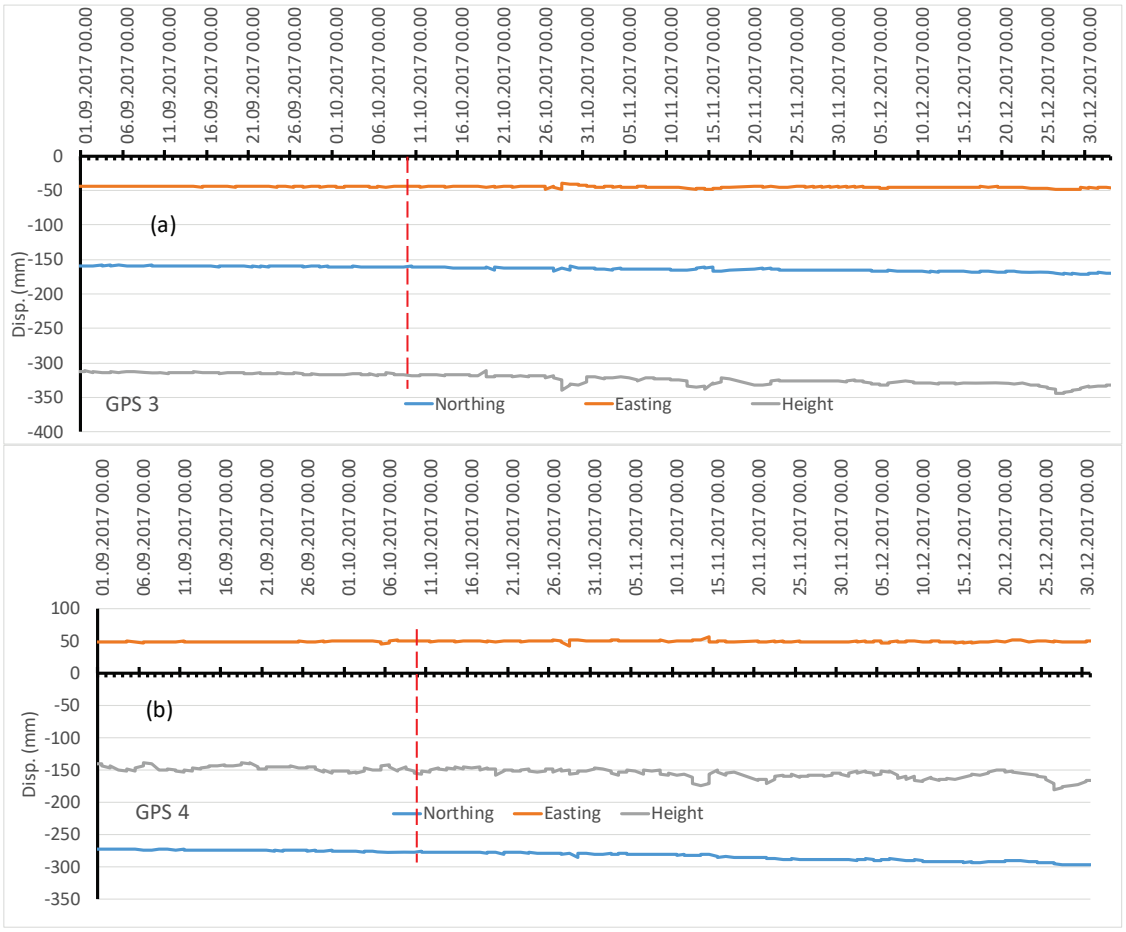

Figure 8. Recorded displacements in (a) GPS-3 and (b) GPS-4. The marked date with red correspond with the highest water head (4 m water standing on the sliding plane) recorded in KH-01-2012 at 10.10.2017.

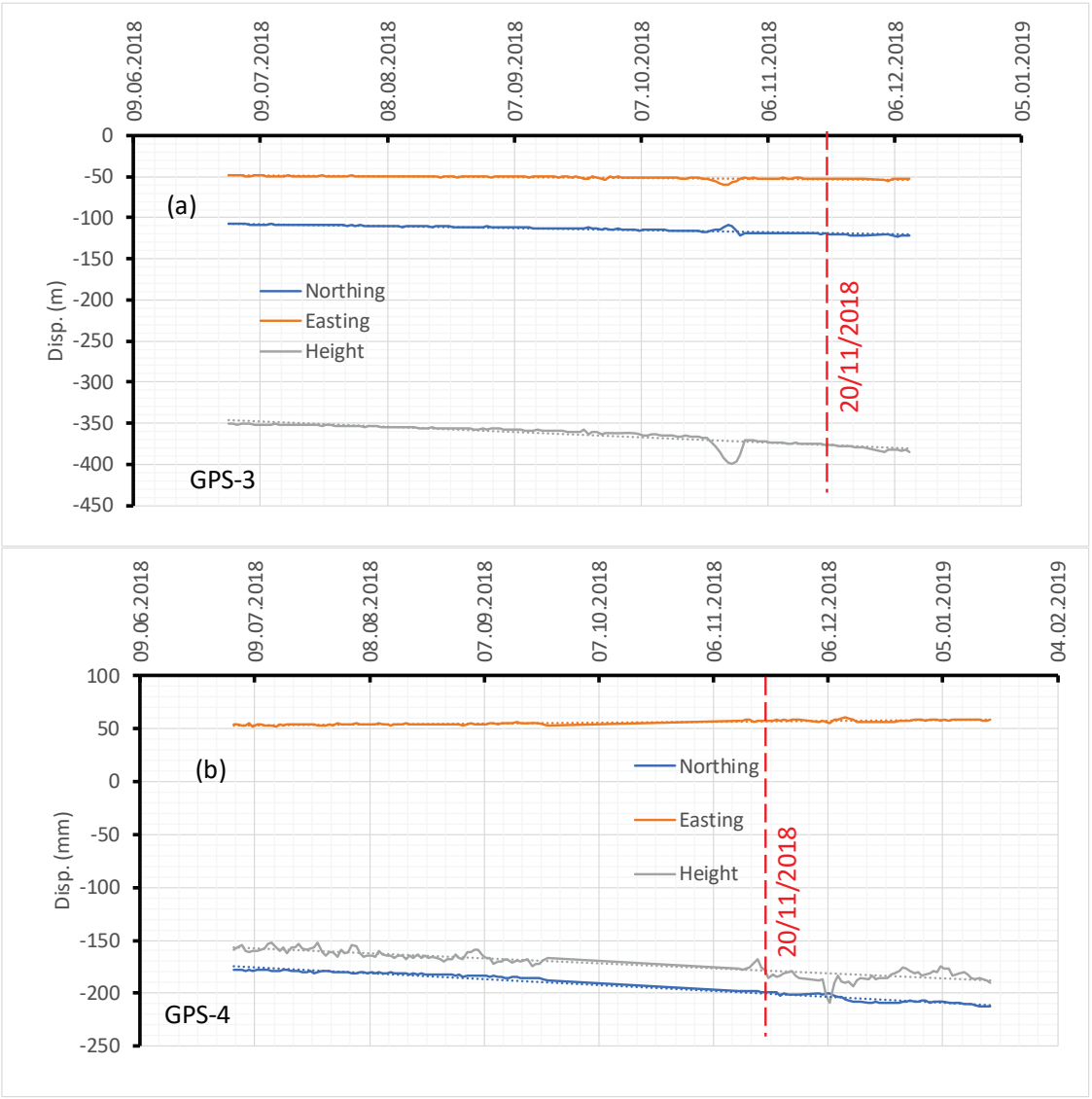

Figure 9. Recorded displacements in (a) GPS-3 and (b) GPS-4. The marked date with red correspond with the second highest water head (1.7 m water standing on the sliding plane) recorded in KH-01-2012 on 20.11.2018.

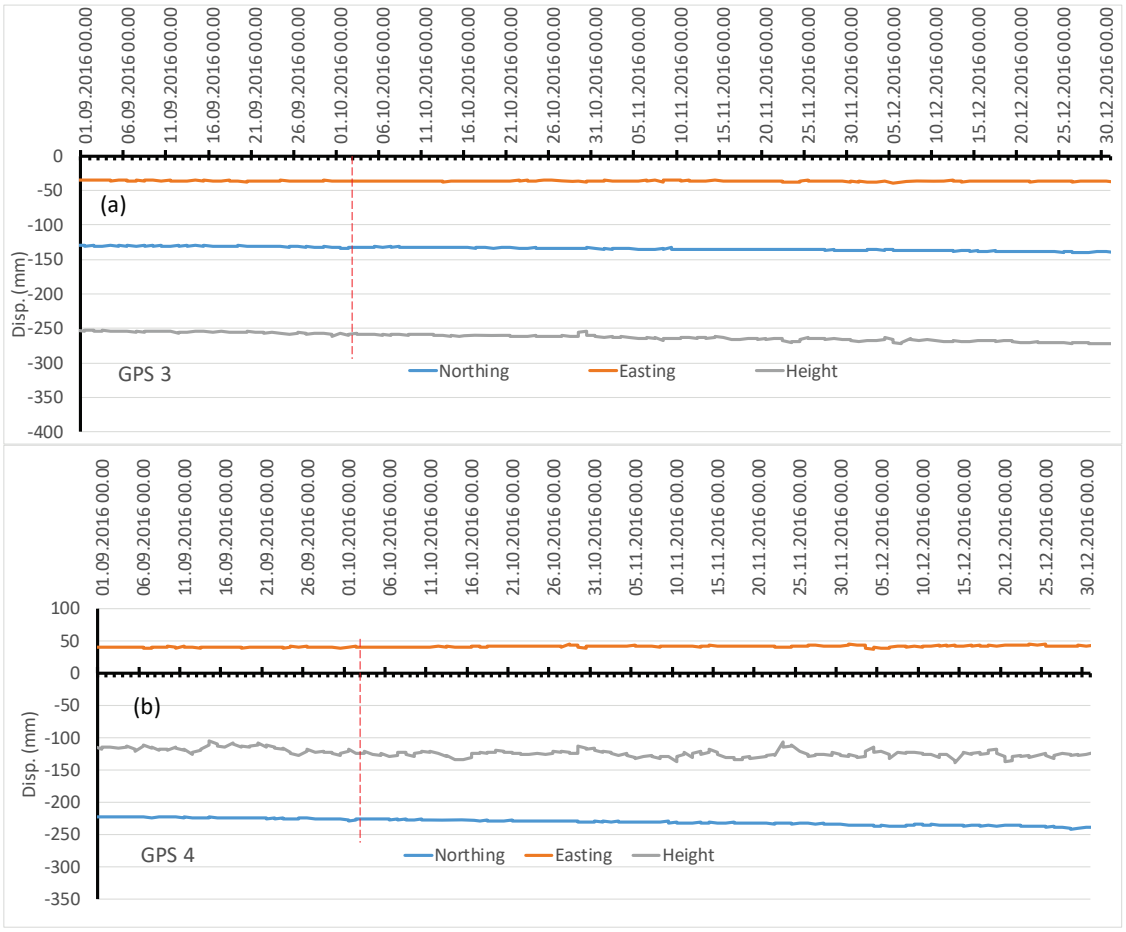

Figure 10. Recorded displacements in (a) GPS-3 and (b) GPS-4. The marked date with red correspond with the third highest water head (1.5 m water standing on the sliding plane) recorded in KH-01-2012 at date of 03.10.2016.

Groundwater head measurements in borehole KH-01-2018 is useable just from 01.01.2020 due to the errors happening after the filling of the packers. Similarly, to the approach presented in section 3.1 of the hydrogeological report [11], the water head at 01.01.2020, 01.02.2020 and 01.03.2020 was extracted from borehole KH-01-2018 and a representative groundwater table was found for those dates.

As we can see from Figure 7 the water table starts to decrease from first December every year towards March. Again, after March the water table starts to increase and reaches the peak value around October / November each year. Hence, water head is descending or constant during first 3 months of the year, as presented in Figure 11. This shows that the water head measurements in both boreholes are corresponding to each other. Moreover, there is no observed acceleration during this period since water head is descending (Figure 12).

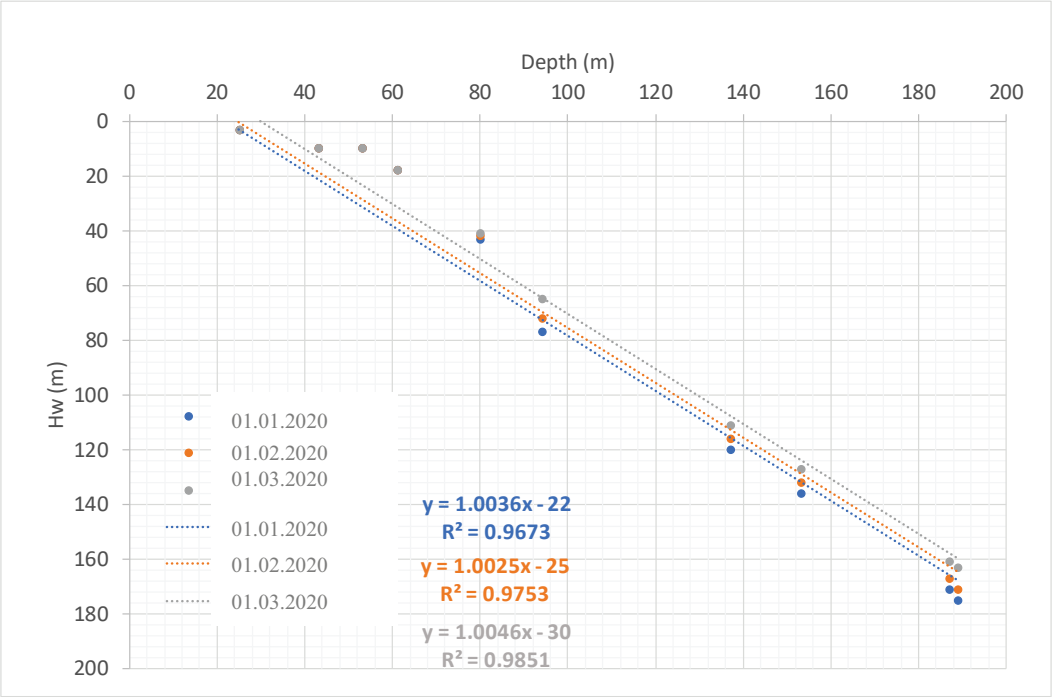

Figure 11. Water head changes in borehole KH-01-2018 during January, February and March 2020.

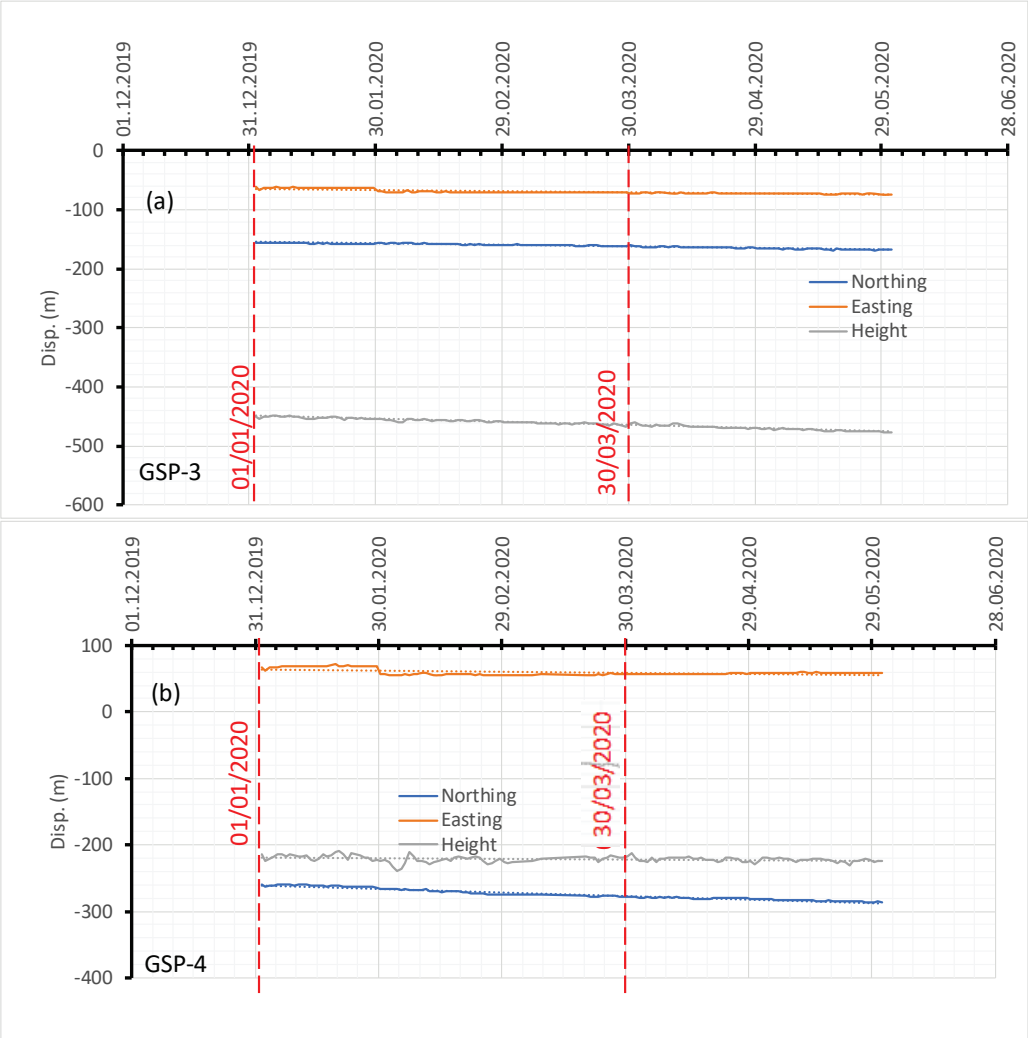

Figure 12. Displacements recorded in (a) GPS-3 and (b) GPS-4 during 01.01.2020 to 30.03.2020.

Based on the mentioned mechanism we suggest following criteria to investigate the correlation of the groundwater fluctuations and slope acceleration:

- Since there are no clear correlations between groundwater fluctuations and precipitation [11], groundwater fluctuations and water pressure on sliding plane should be correlated with displacement, not precipitation rate.
- Increase in water head leads to decrease of normal stress on the sliding plane. Build-up of water pressure on and above sliding plane should be correlated with displacement in the specific section with detected sliding plane.

7 Geological cross-sections for numerical modelling

For the 2D stability analysis, it is required to have geological cross-sections which shows location of the sliding planes and the geology around it. So far two different geo-models have been suggested for

Åknes rock slide Ganerød et al. 2008 [7] and Jaboyedoff et al. 2011 [8]. Since both models were developed with less data than today, it is natural to consider their uncertainties before using them. Based on the knowledge from those two suggested geo-models and current observations, geological cross-sections for the Åknes rock slide will be suggested.

7.1 Available geo-models

Initial model was suggested by Ganerød et al. (2008). Figure 13 shows the suggested model and a cross-section along the slope. The Åknes rock slope area is defined by the prominent 500-meter-long back scarp at 900 meter above sea level (masl), a deep valley and a fault as western and eastern limits, respectively, and the toe zone that outcrops at about 100 masl. The sliding zones delimit the moving slope in depth, daylighting at different levels in the slope. Four domains were identified in the sliding body.

The well-developed foliation in the rock mass is intensely folded at the head scarp but dips subparallel to the topographic slope downslope. Biotite-rich layers, with up to 20 cm thickness, is oriented parallel to the foliation and represent zones with high fracture frequency. These geological features are probably closely linked to the large-scale displacement and enables formation of tension fractures along the back scarp and sliding on weak layers downslope.

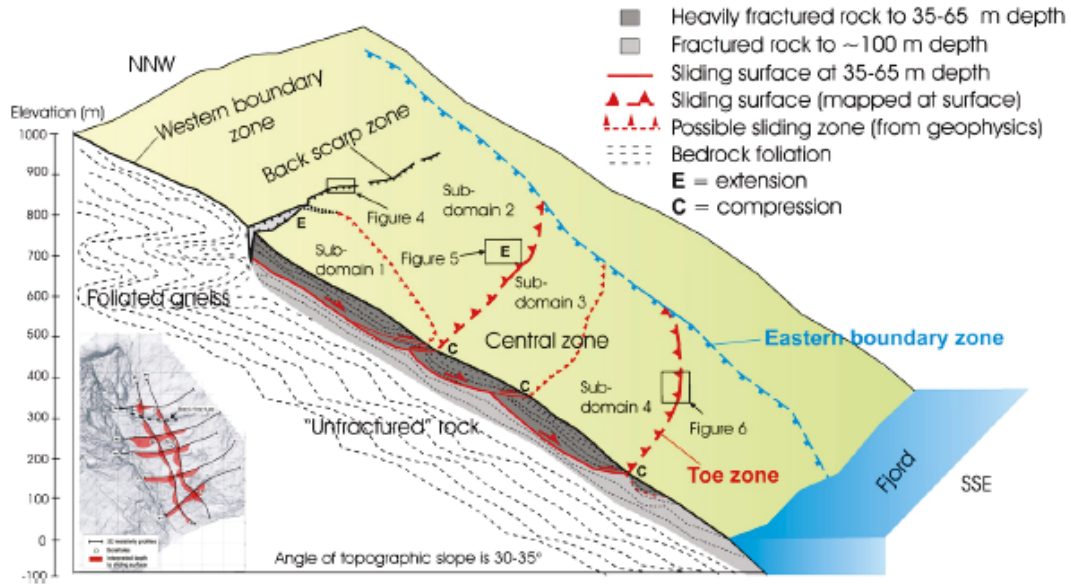

Figure 13. Geo-model suggested by Ganerød et al. (2008).

Second model was suggested by Jaboyedoff et al. (2011). The model identifies that extension processes generated the backscarp due to sub-vertical isoclinal folding, is repeated at several topographical ridges downslope from the backscarp (brown sub-vertical planes in Figure 14). Both the sub-vertical extension fracturing and existing shearing zones control movements of the slope, generating a stepped sliding surface. They also argued that undulation of the foliation joints lead to two different sliding directions in the Åknes rock slide.

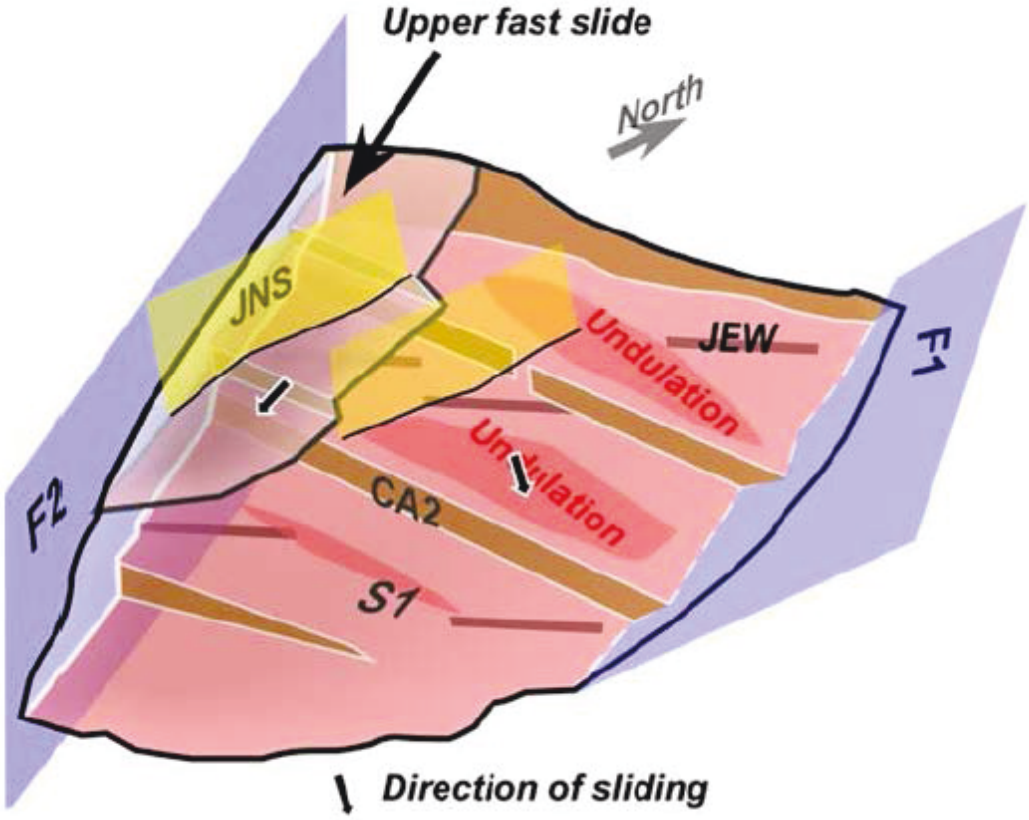

Figure 14. Conceptual model of the unstable slope at Åknes. From Jaboyedoff et al. (2011).

Both models identify two directions of movement in the western and eastern part of the slope.

Both models considered a toe area at elevation of about 150 masl. showing uplift movement. They assumed that the toe area is under compression from the unstable mass moving in higher elevations without providing any evidence from neither structural geology point of view nor kinetics point of view.

7.2 Suggested geological cross-sections for numerical modelling

Long-term monitoring of the slope has revealed that there is no movement in the toe area (located at about 150 masl.) in contrast to Ganerød et al. (2008) and Jaboyedoff, et al. (2011). GPS 8 and 9 show that there are vertical fluctuations in the ground which follows the atmospheric temperature. They show expansion and contraction in summer and winter temperature, respectively.

To develop geological cross-sections, a systematic approach was followed:

1. The location of the sliding planes was marked with considered DMS data.
2. The sliding planes were confirmed by cores from the boreholes.
3. The sliding plane extrapolated between boreholes located on same cross-sections with considering geophysical measurements, that is provided by NVE in the Petrel model.

4. The tension crack at the back of the slope (back scarp) was considered as the upper boundary of the slope.

Extrapolating the data from sliding planes marked by boreholes, electrical resistivity and backscarp toward toe reveal that the toe of the sling mass is located almost at the elevation of the springs marked around 450 – 400 masl (Figure 15 and 16).

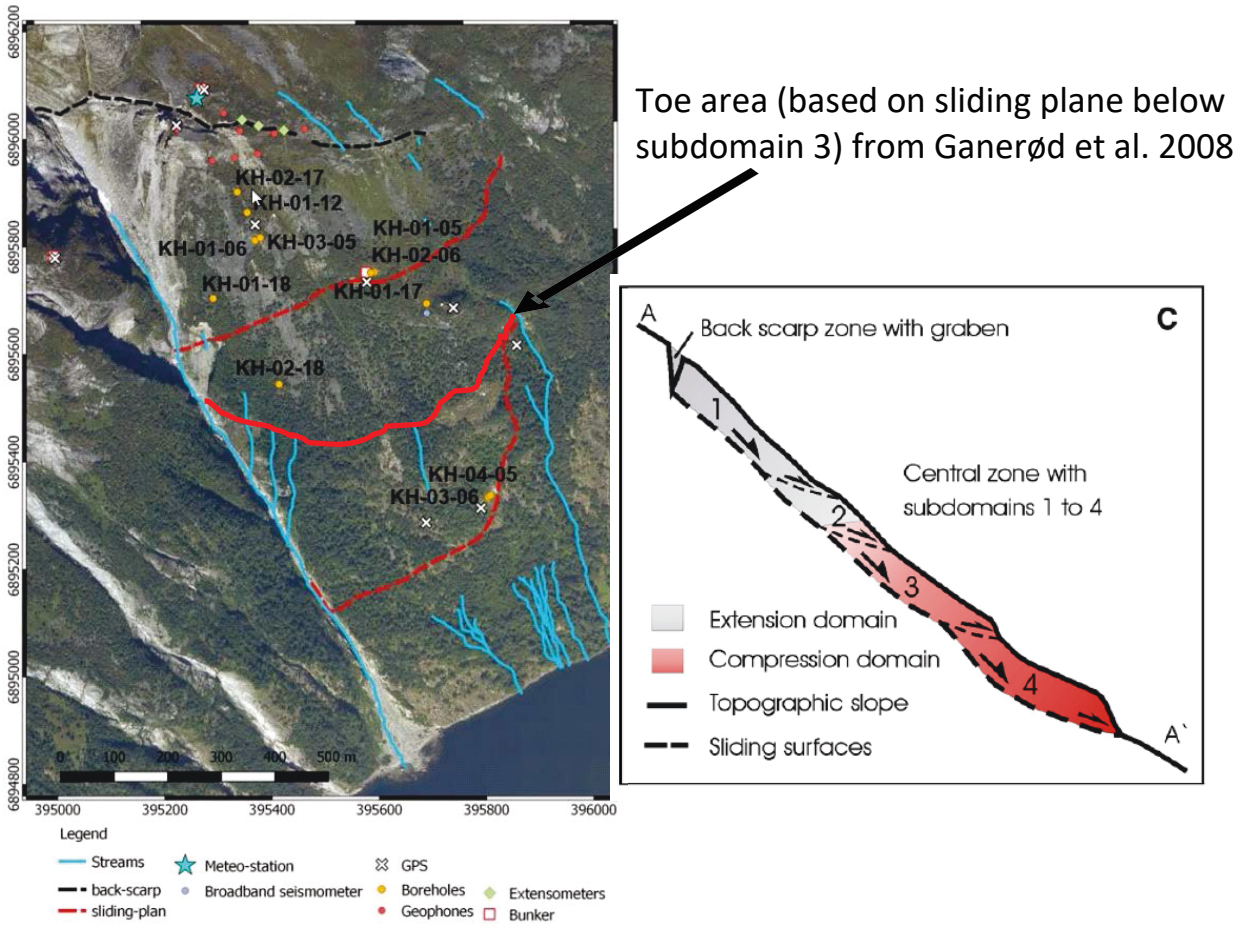

Figure 15 Illustration presenting location of boreholes, GPS, geophones, extensometer as well as suggested location of two sliding planes (dotted red lines) and one sliding plane in the middle (red line) and registered streams (modified from Clara Sena's presentation, 28. Nov 2019).

The suggested geological cross-sections for the numerical modelling are presented in Appendix D.

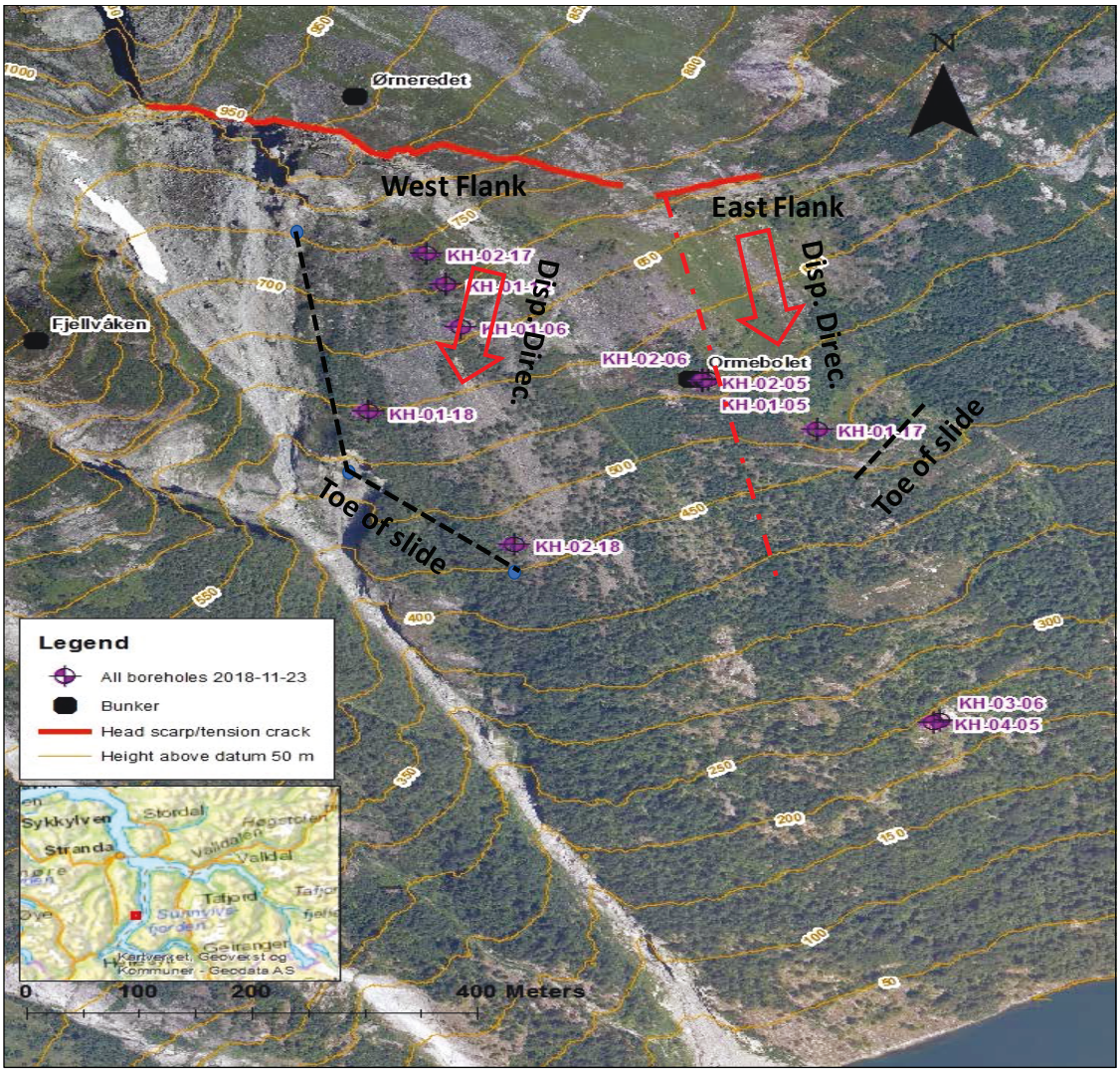

Figure 16. Illustration of possible locations of local toe areas in the rock slope.

8 Concluding remarks

Comparing displacement – time curves from the GPS data shows continuous linear displacement over the entire rock slope. Highest displacements are registered in the West flank with mean velocity for GPS4 (Oct 2011 to Sept 2018) of 0,14 mm/day and 0,13 mm/day for total and horizontal velocity respectively. An interesting observation is that for the north-western part (block 8 in Kveldsvik et al. 2008) the analysis of old surface displacements shows a trend with decreasing displacements (See Chapter 6.2). Photogrammetry from 1961 to 1983 gives mean horizontal displacement of 0,35 mm/day for GPS3. And between 1983 and 2004 the mean horizontal velocity was 0,21 mm/day. From this the conclusion is that the displacements at the surface in block 8 is decreasing. New data from block 8 should be analysed in the future.

The West flank is showing a regressive or transitional behaviour, either following curve A or C in Figure 3. The north-western area of the rock slope has shown a regressive period from 1961 until today.

Åknes has two different main blocks, East and west flank, with different movement patterns independent from the other. Therefore, in case of acceleration of the unstable mass, it should be studied separately. The rock slope may be divided in more than 10 blocks which have different behaviour and movement patterns (Kveldsvik et al. 2008) [6]. Behaviour in West and East flank should be analysed separately. Water head in a section of a borehole in East flank cannot be related to acceleration on the West flank. This report has not focused on finding different movement patterns. Rather to find the most critical areas for numerical modelling. Therefore, it was decided to start with a profile in the north-western part, Profile W2, of Åknes rock slope, see Appendix D for details on location of this profile.

9 References

[1] Wyllie D.C., Mah C.W. (2004). Rock slope engineering: civil and mining, edition: 4. Spon Press, Taylor and Francis Group.

[2] Jaeger JC, Cook NGW, Zimmerman R (2007). Fundamental of rock mechanics, edition: 4. Wiley-Blackwell.

[3] Atkinson B.A. (1987). Fracture mechanics of rock. Elsevier Ltd., Doi: https://doi.org/10.1016/C2009-0-21691-6 .

[4] Sullivan T.D. 2007 Hydromechanical Coupling and Pit Slope Movements, Australian Centre for Geomechanics, Perth, ISBN 978-0-9756756-8-7, 41 pp.

[5] Ryan T.M., Call R.D. Applications of rock mass monitoring for stability assessment of pit slope failure. In: Proceedings of the 33th U.S. Symposium on Rock Mechanics (USRMS). Santa Fe; 1992. p. 221-229.

[6] Kveldsvik, V. Einstein, H.H., Nilsen, B. and Blikra, L.H. 2008: Numerical Analysis of the 650,000 m^2 Åknes Rock Slope based on Measured Displacements and Geotechnical Data. Rock Mech Rock Eng (2009) 42: p. 689-728

[7] Green G.E., Mikkelsen P.E. 1998: Deformation measurements with inclinometers. Transportation research record (1998) 1169 (15 p).

[8] NGU, 2007. Logging of drill cores from seven boreholes at Åknes, Stranda municipality, Møre and, Trondheim, Norge: Norges Geologiske Undersøkelse.

[9] Ganerød, G.V., Grøneng, G., Rønning, J.S., Dalsegg, E., Elvebakk, H., Tønnesen, J.F., Kveldsvik, V., Eiken, T., Blikra, L.H. and Braathen, A. 2008: "Geological model of Åknes rock slide, western Norway" Engineering Geology (102) 2008 p. 1-18.

[10] Jaboyedoff, M. et al., 2011. Complex landslide behaviour and structural control: A three-dimensional conceptual model of Åknes rockslide, Norway. I: *Slope Tectonics.*. London: The Geological Society of London, Special Publications 6.1.1.

[11] NGI (2020), Åknes rock slope: Hydrogeological report, Report No. 20180662-06-R, revision 00.

Appendix A

VELOCITY AND ACCELERATION FROM GPS DATA

GSP-3 Total overview

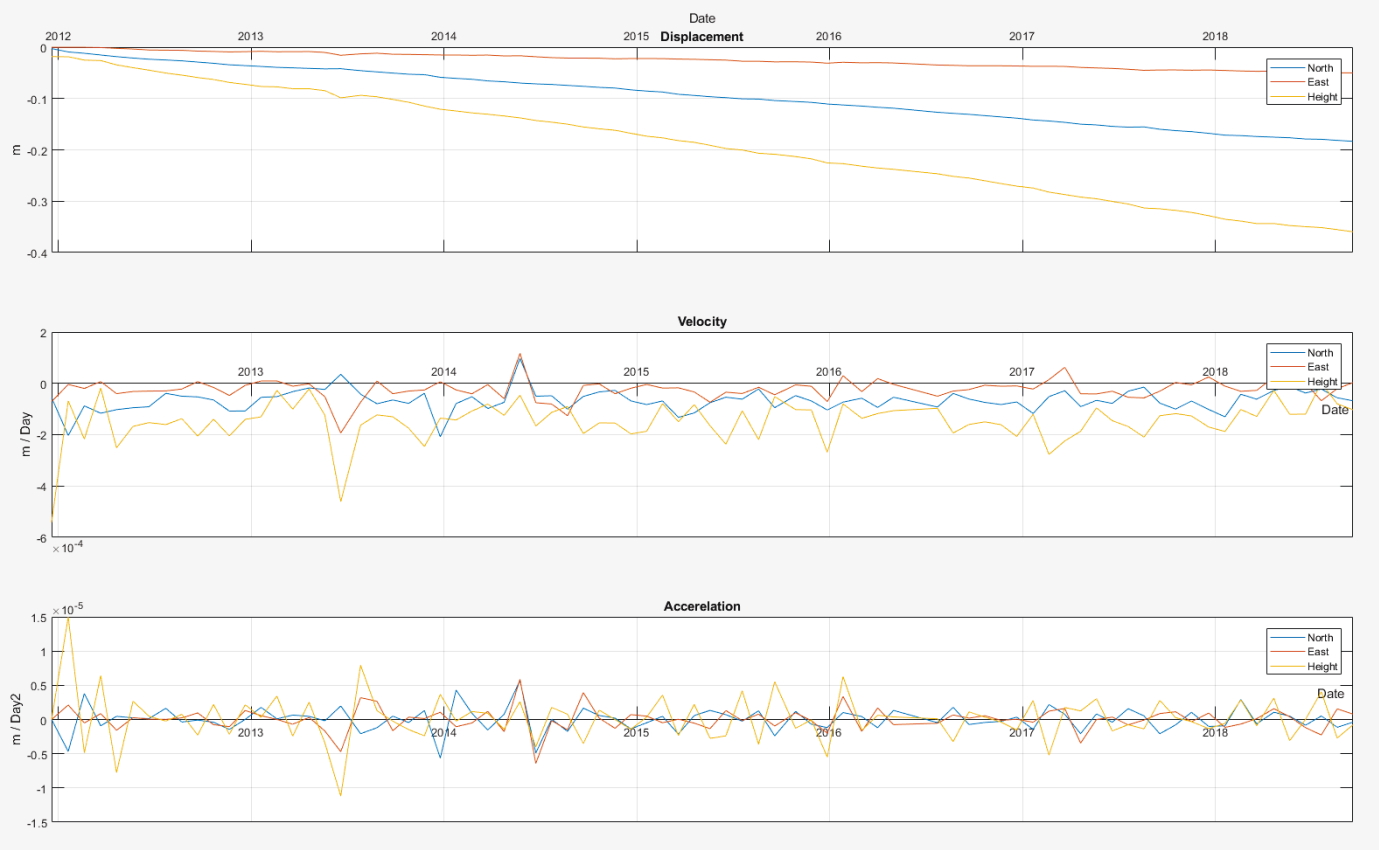

GSP-3 Velocity and acceleration in East and North directions

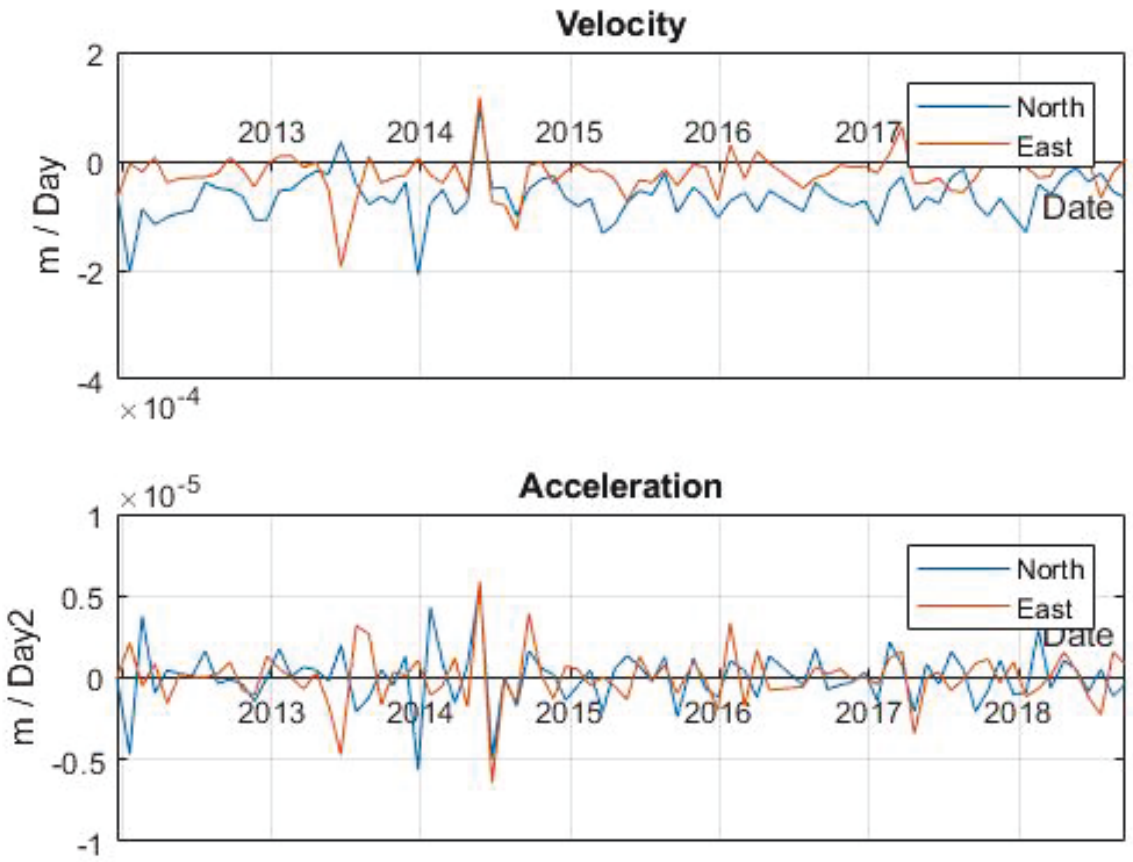

GSP-4 Total overview

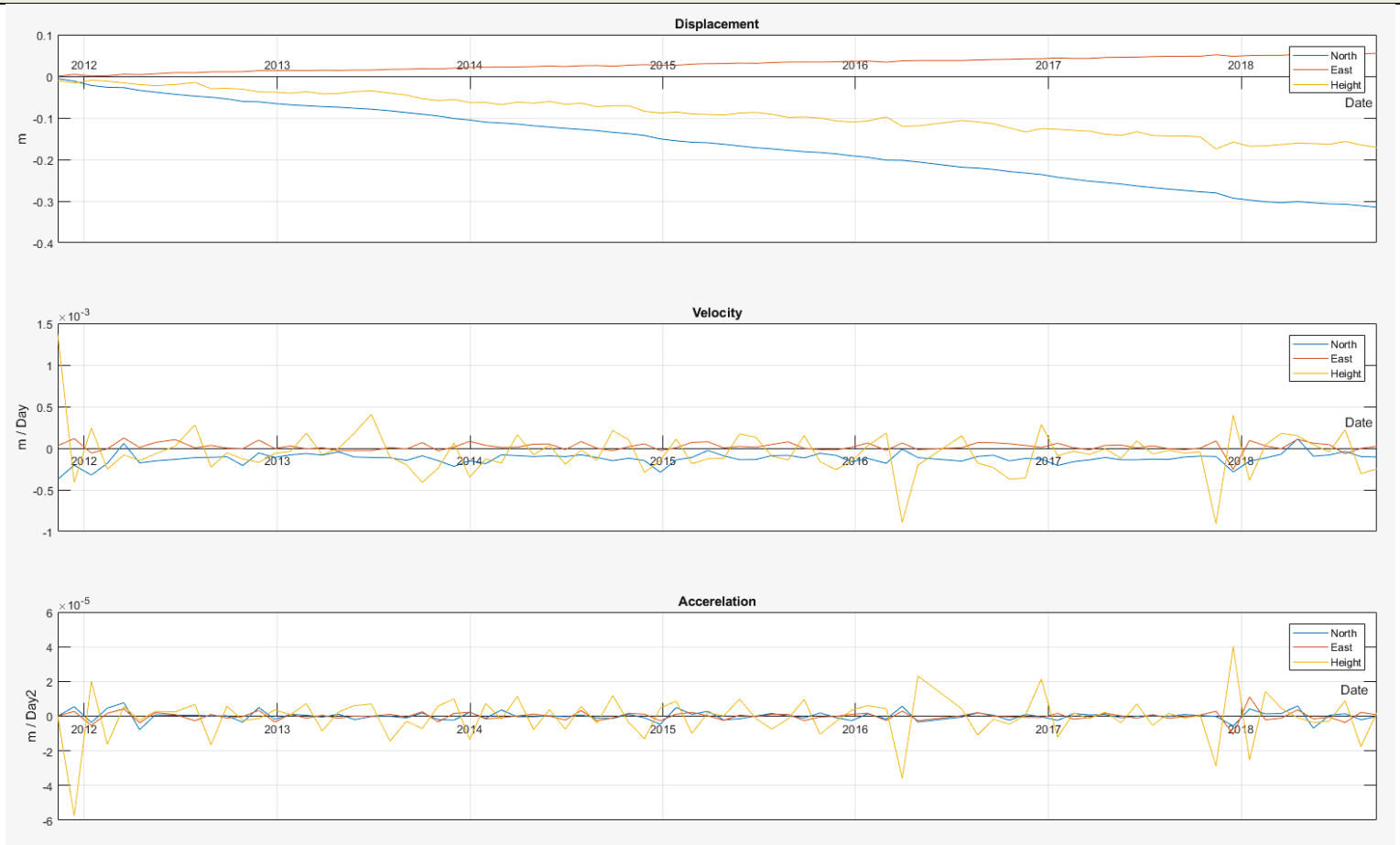

GSP-4 Velocity and acceleration in East and North directions

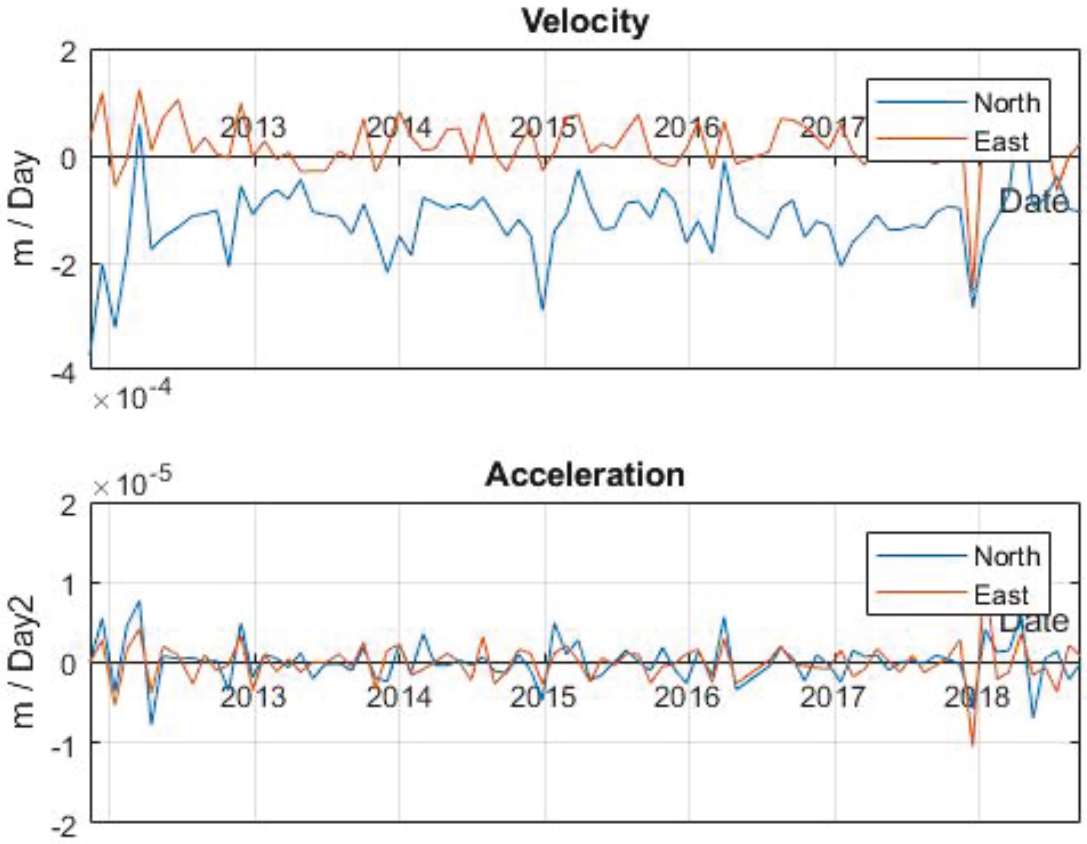

GSP-5 Total overview

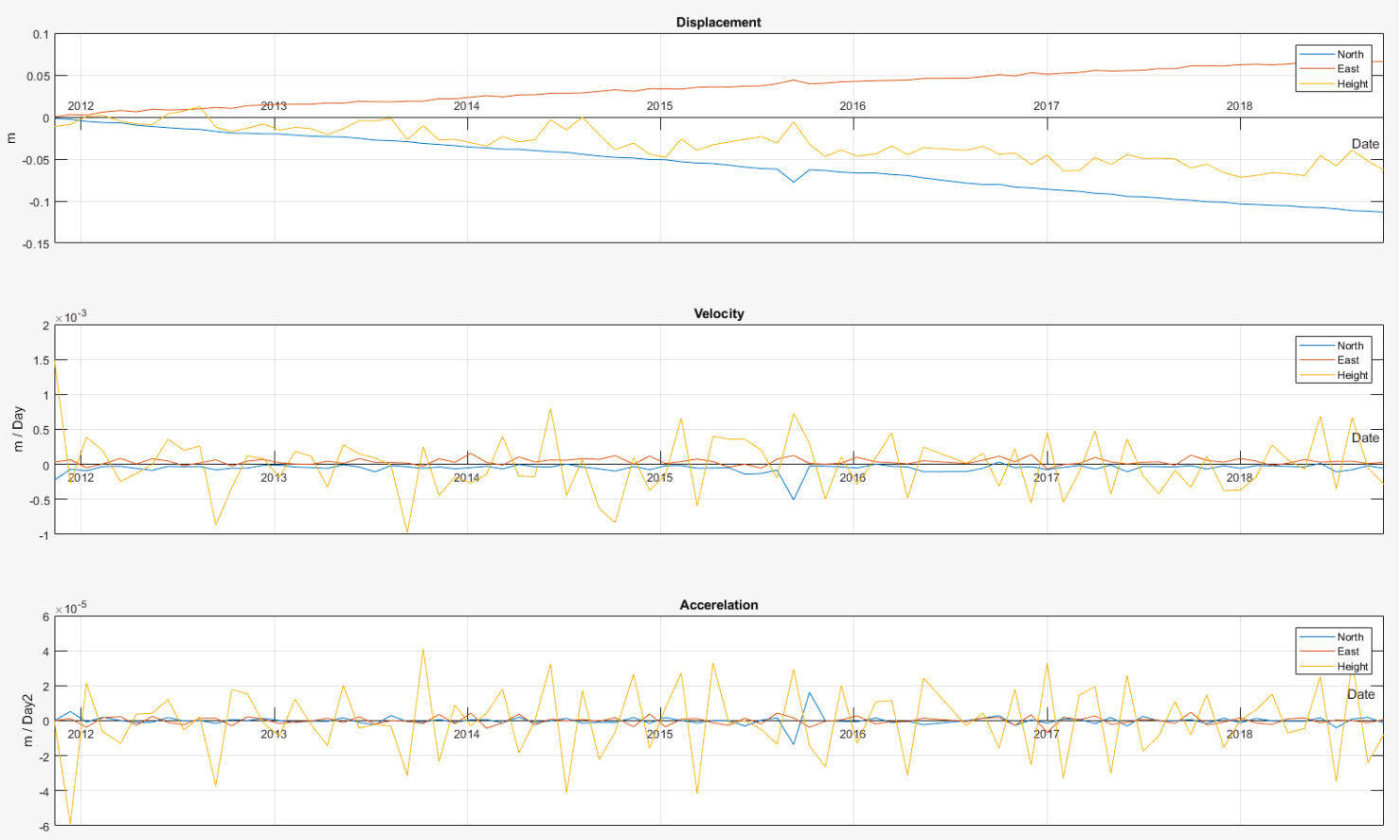

GSP-5 Velocity and acceleration in East and North directions

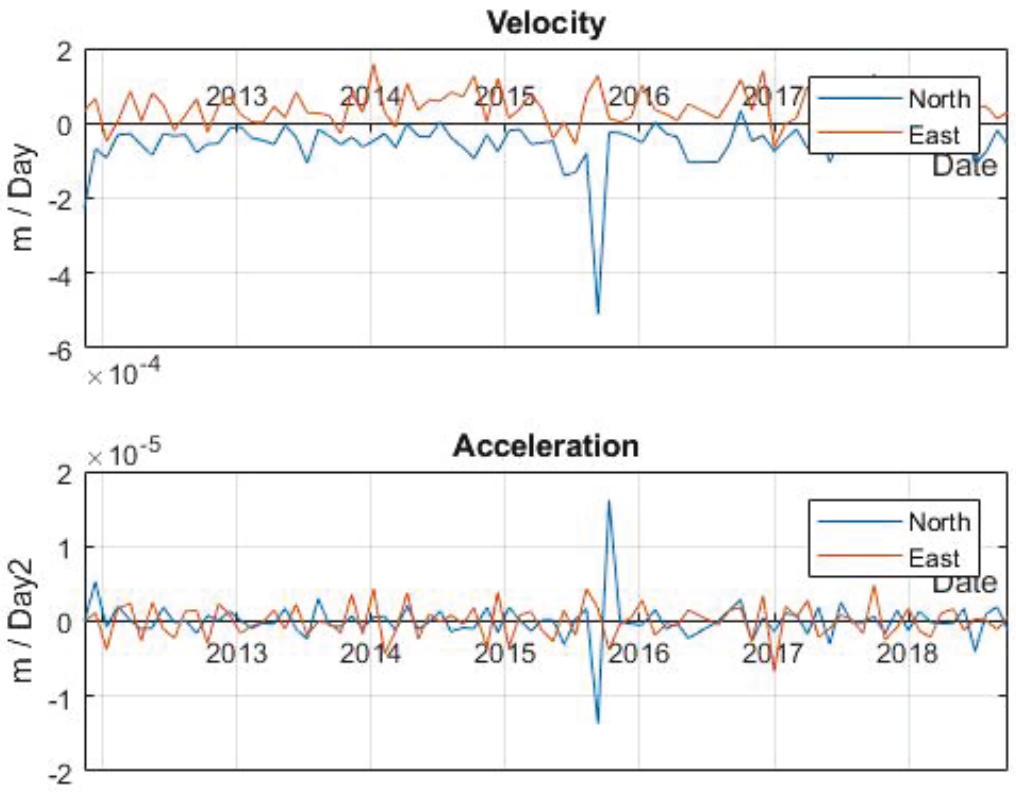

GSP-6 Total overview

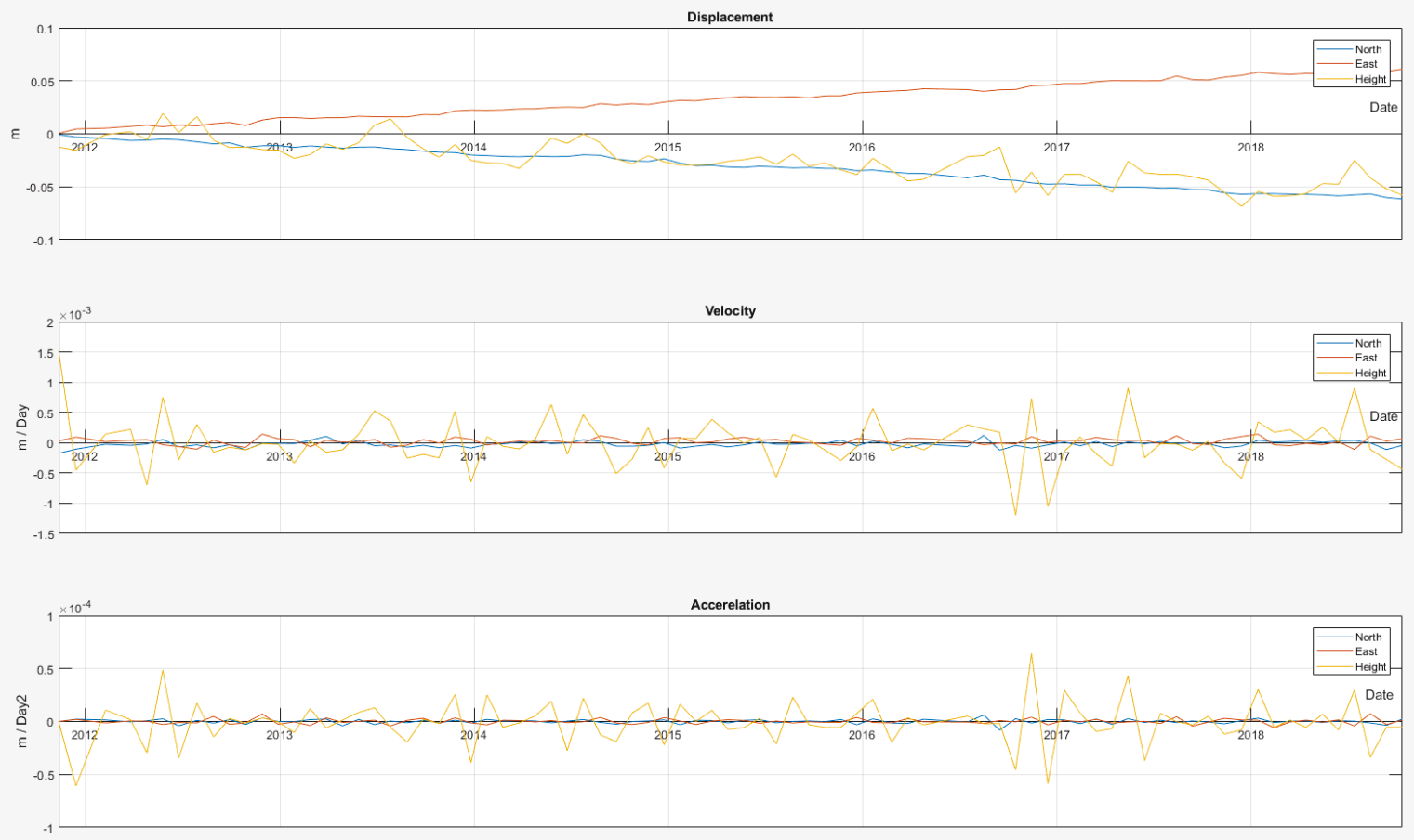

GSP-6 Velocity and acceleration in East and North directions

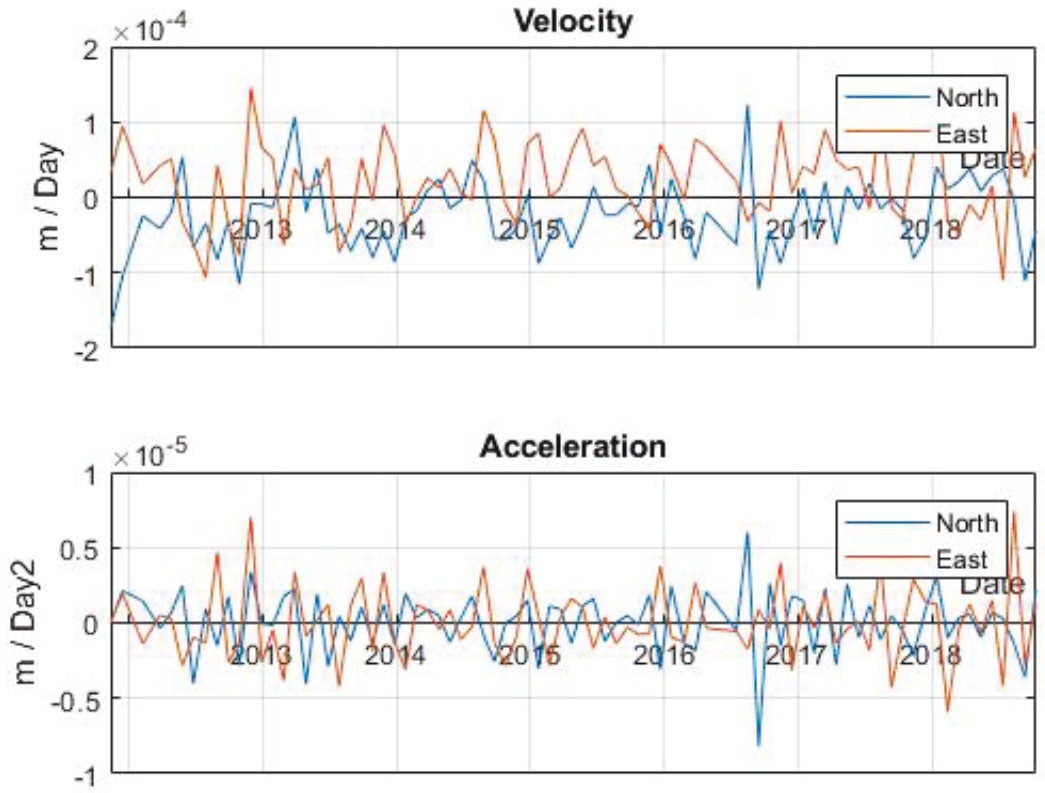

GSP-7 Total overview

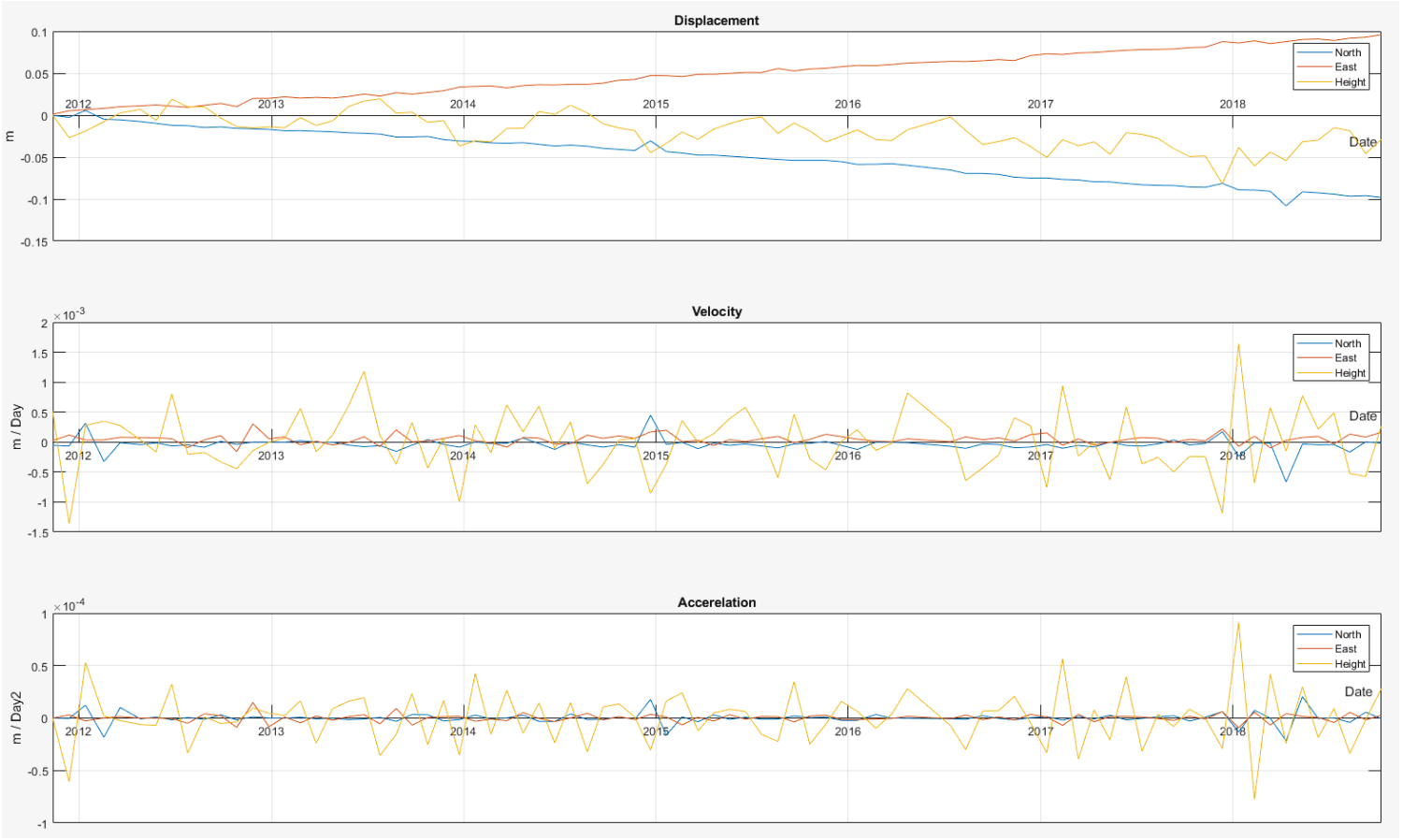

GSP-7 Velocity and acceleration in East and North directions

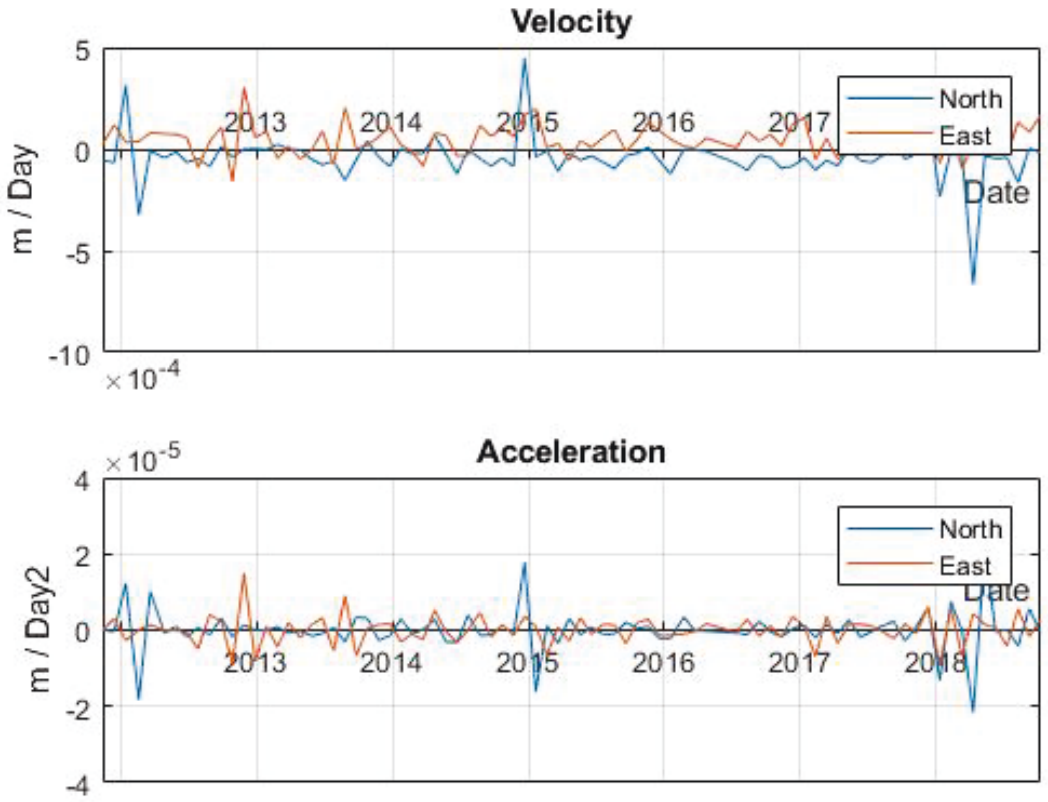

GSP-8 Total overview

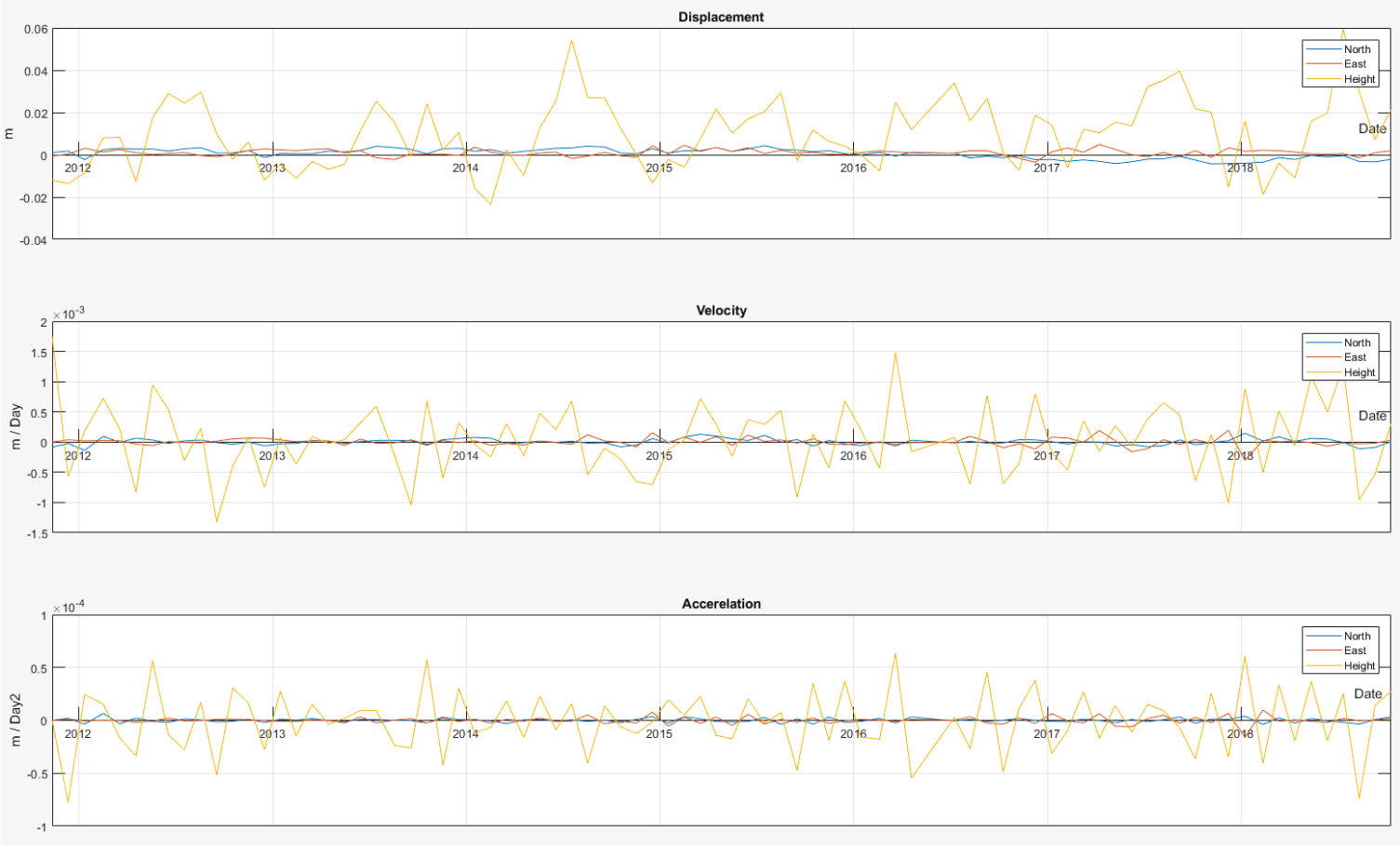

GSP-8 Velocity and acceleration in East, North and vertical directions

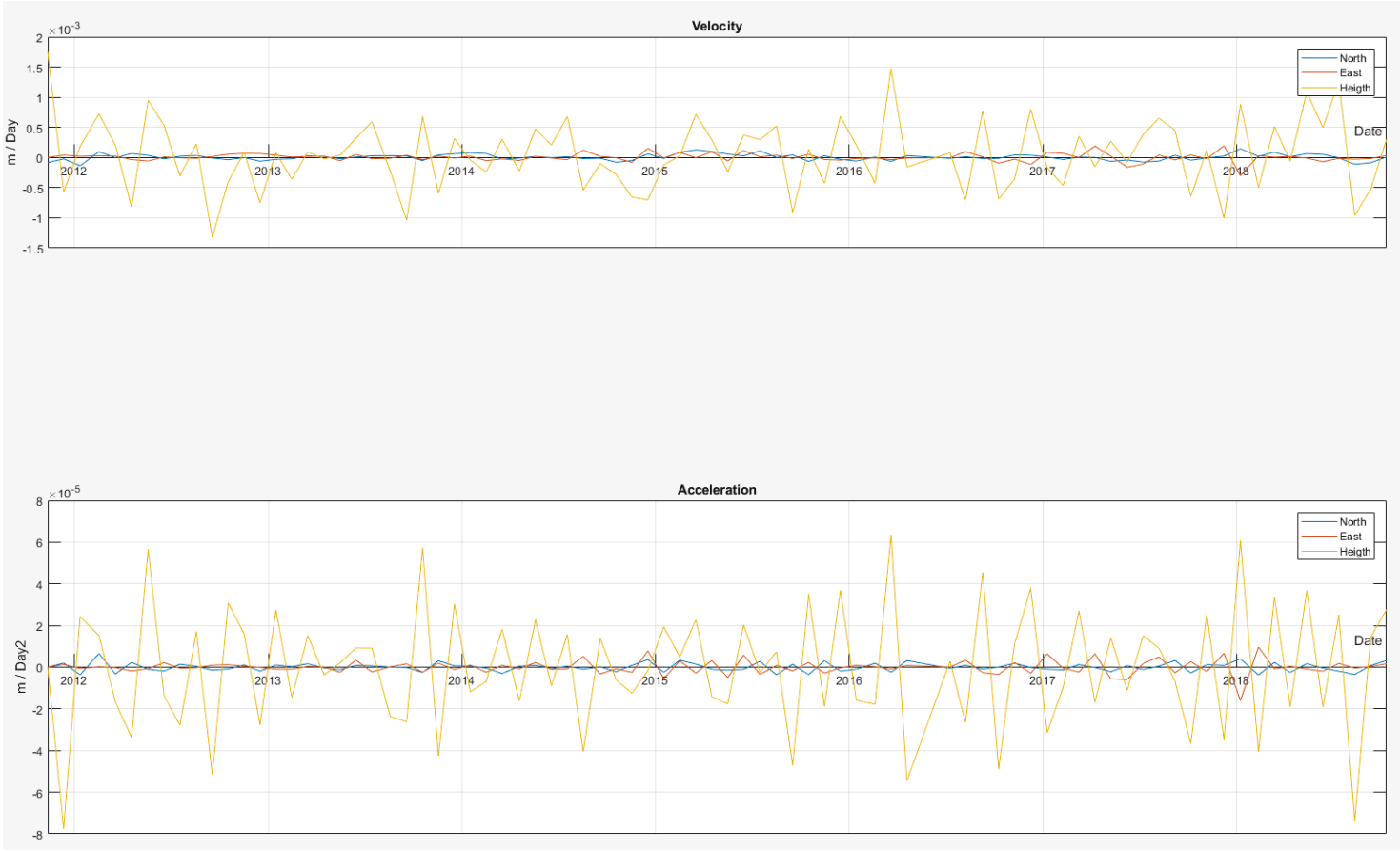

GSP-9 Total overview

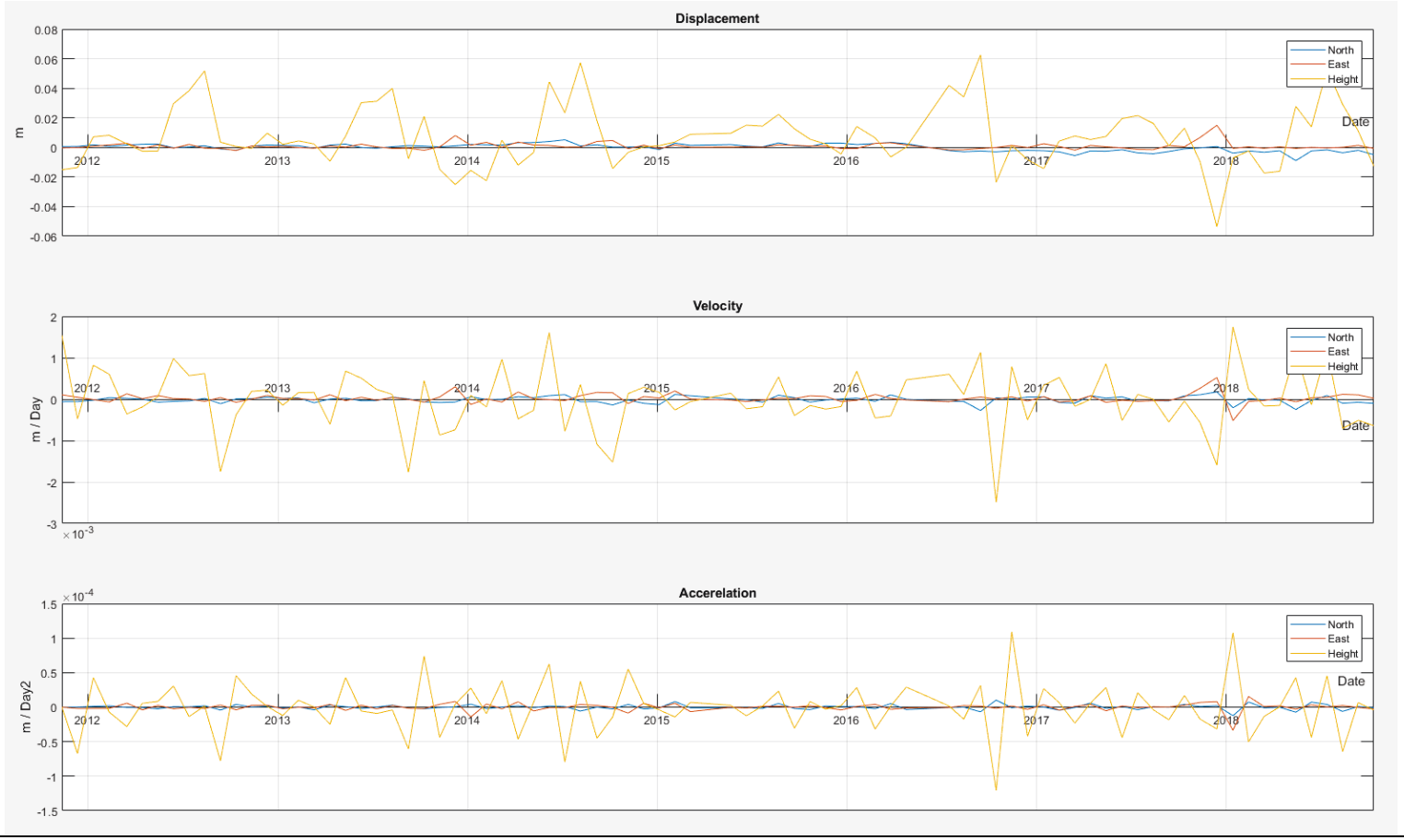

GSP-9 Velocity and acceleration in East, North and vertical directions

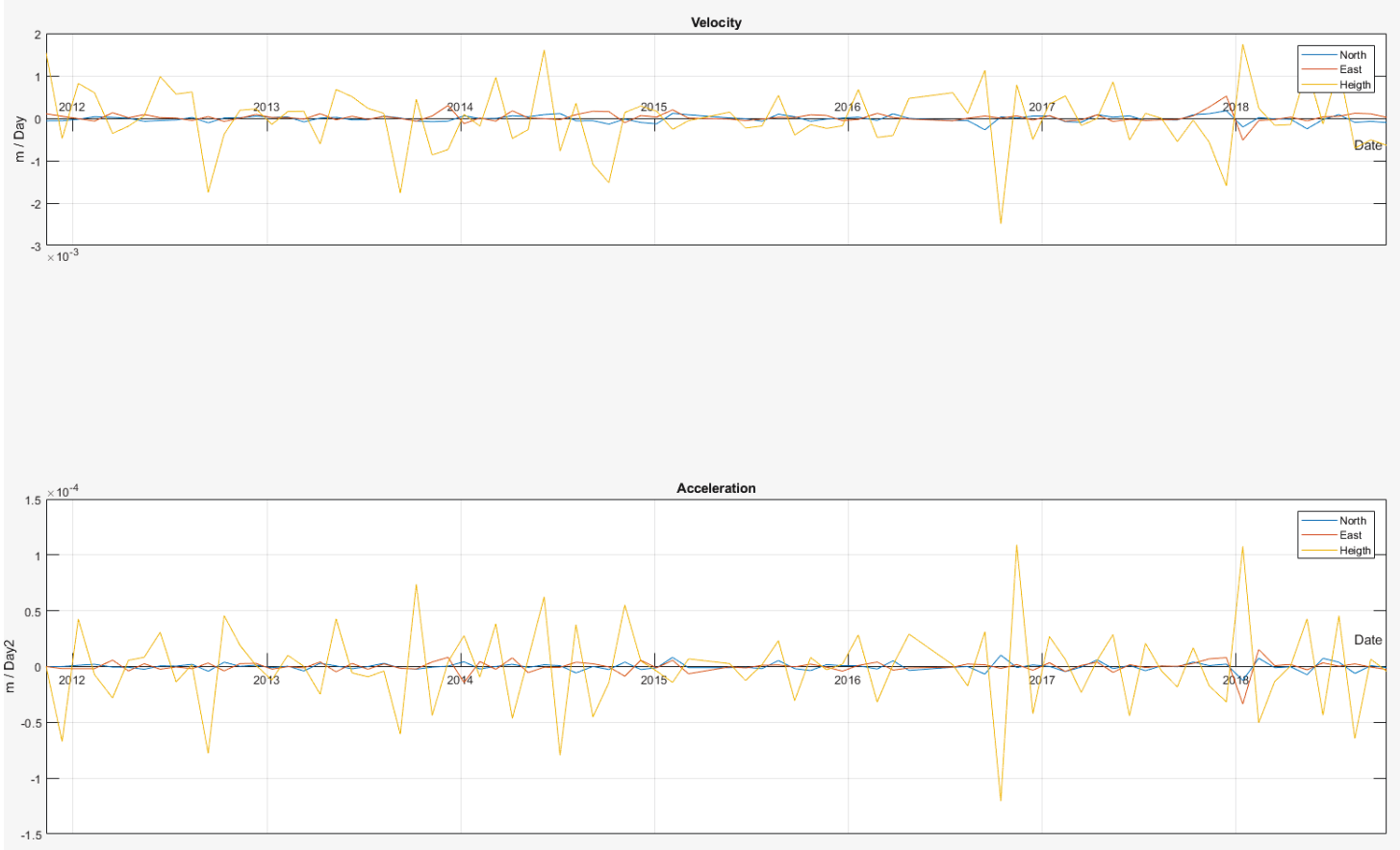

Appendix B

CORRELATIONS BETWEEN DMS MEASUREMENTS AND CORE PICTURES / CORE LOGS

Borehole KH-02-2006

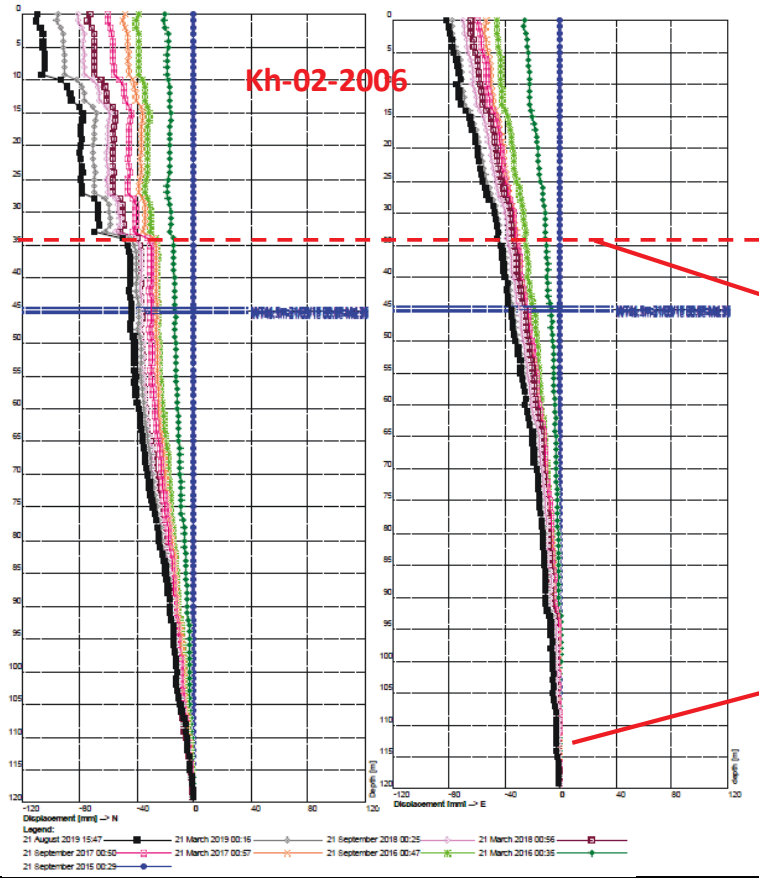

Depth (m)	Bedrock type	Ca % content of mafic minerals (biotite)	Zones	Core loss [cm]	Crushed rock [cm]	*Fracture frequency	** Effective Fracture frequency	Foliation parallel fractures	Other fractures
-12	GG	30			5	7	7	0	
-13	GG	30			16	7	11	6	
-14	GG to BG	30				7	7	5	
-15	BG	60				12	15	6	
-16	GG/BG	30				5	5	2	
-17	GG to BG	40			15	6	15	3	
-18	BG/GG	30				2	2	1	
-19	GG/BG	40			3	7	7	4	
-20	GG	5			25	7	16		
-21	GG	10			4	3	6		
-22	GG/BG	50				9	9		
-23	GG/BG	50			6	17	21	12	
-24	BG	60				21	21	16	
-25	BG	60				15	15	15	
-26	BG	60				14	14	12	
-27	BG	60				14	14	9	
-28	BG	60			15	13	23	11	
-29	BG to GG	30				8	15	8	
-30	GG	10				6	6	3	
-31	GG	10				7	7	7	
-32	GG	10				2	2	2	
-33	GG	10		75		2	2	2	
-34	GG to BG/BG	78-80			32	9	50	20	
-35	BG/GG	30				8	8	6	
-36	GG with B-bands	20				9	9	6	
-37	GG to DG	40				9	9	2	
-38	GG with chlorite	30				10	10	2	
-39	GG with chlorite	30				7	7	2	
-40	GG with chlorite	30				6	6	4	
-41	GG with B-bands	40				6	6	3	
-42	BG	40				12	12	11	
-43	GG to BG	50				10	10	9	

Depth (m)	Bedrock type	Ca % content of mafic minerals (biotite)	Zones	Core loss [cm]	Crushed rock [cm]	*Fracture frequency	** Effective Fracture frequency	Foliation parallel fractures	Other fractures
-102	BG with Qtf-lenses	50				9	9	6	
-103	BG with Qtf-bands	50				8	8	6	
-104	BG with Qtf-bands	60				8	18	17	
-105	BG with chlorite	60				2	2	1	
-106	BG with chlorite	60				6	6	3	
-107	BG with chlorite	60				4	4	3	
-108	BG with chlorite	60				5	5	3	
-109	BG with chlorite	60				4	4	4	
-110	peg/BG	50				9	9	6	
-111	BG	60				9	9	7	
-112	GG	50				9	9	4	
-113	GG til BG	50				7	7	5	
-114	GG til BG	60				4	4	2	
-115	GG	50				3	3	2	
-116	GG/BG	50				4	4	2	
-117	GG til BG	60				6	6	6	
-118	GG til BG	60				6	6	5	
-119	GG	60				5	5	4	

Borehole KH-03-2006

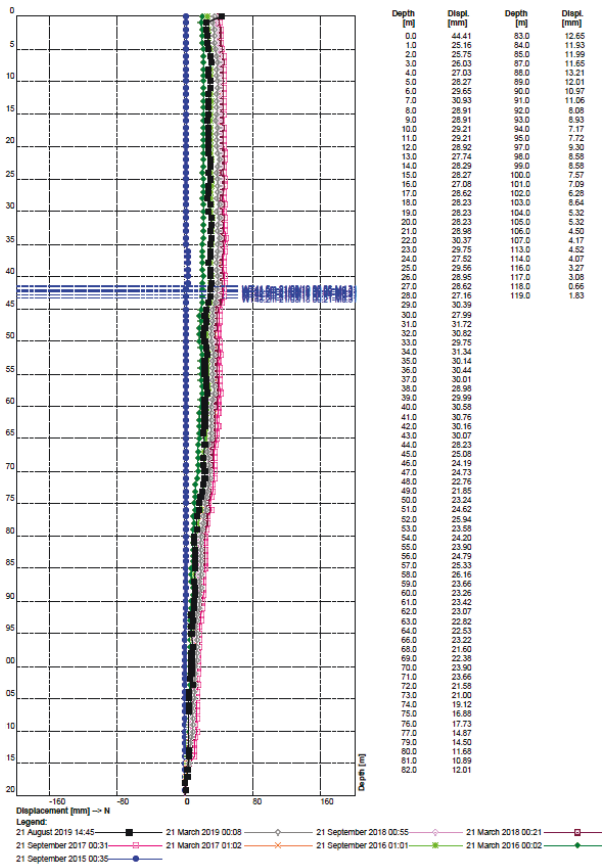

Depth [m]	Displ. [mm]	Depth [m]	Displ. [mm]
0.0	44.41	83.0	12.65
1.0	25.16	84.0	11.93
2.0	25.75	85.0	11.99
3.0	26.03	87.0	11.65
4.0	27.03	88.0	13.21
5.0	28.27	89.0	12.01
6.0	29.65	90.0	10.97
7.0	30.93	91.0	11.06
8.0	28.91	92.0	8.08
9.0	28.91	93.0	8.93
10.0	29.21	94.0	7.17
11.0	29.21	95.0	7.72
12.0	28.92	97.0	9.30
13.0	27.74	98.0	8.58
14.0	28.29	99.0	8.58
15.0	28.27	100.0	7.57
16.0	27.08	101.0	7.09
17.0	28.62	102.0	6.28
18.0	28.23	103.0	8.64
19.0	28.23	104.0	5.32
20.0	28.23	105.0	5.32
21.0	28.98	106.0	4.52
22.0	30.37	107.0	4.17
23.0	29.75	113.0	4.52
24.0	27.52	114.0	4.07
25.0	29.56	116.0	3.27
26.0	28.95	117.0	3.08
27.0	28.62	118.0	0.66
28.0	27.16	119.0	1.83
29.0	30.39		
30.0	27.99		
31.0	31.72		
32.0	30.82		
33.0	29.75		
34.0	31.34		
35.0	30.14		
36.0	30.44		
37.0	30.01		
38.0	28.98		
39.0	29.99		
40.0	30.58		
41.0	30.76		
42.0	30.16		
43.0	30.07		
44.0	28.23		
45.0	25.08		
46.0	24.19		
47.0	24.73		
48.0	22.76		
49.0	21.85		
50.0	23.24		
51.0	24.62		
52.0	25.94		
53.0	23.58		
54.0	24.20		
55.0	23.90		
56.0	24.79		
57.0	25.33		
58.0	26.16		
59.0	23.66		
60.0	23.26		
61.0	23.42		
62.0	23.07		
63.0	22.82		
64.0	22.53		
66.0	23.22		
68.0	21.60		
69.0	22.38		
70.0	23.90		
71.0	23.66		
72.0	21.58		
73.0	21.00		
74.0	19.12		
75.0	16.88		
76.0	17.73		
77.0	14.87		
79.0	14.50		
80.0	11.68		
81.0	10.89		
82.0	12.01		

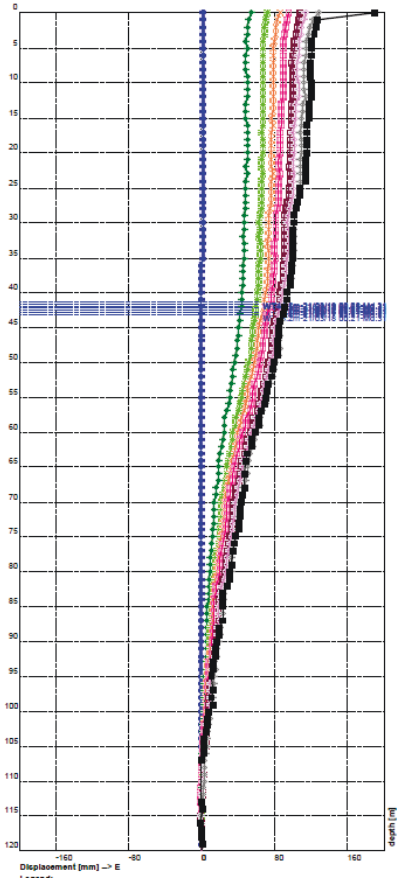

Depth (m)	Bedrock type	Ca % content of mafic minerals (biotite)	Zones	Core loss [cm]	Crushed rock [cm]	*Fracture frequency	** Effective Fracture frequency	Foliation parallel fractures	Other fractures	Fracture angle
-10	BG to GG	50				9	11	7		60; F(25)
-11	GG	50				15	25	15		irreg;45; 90; F(20-45)
-12	GG/BG to GG	60				5	5	4		90; F(15;25)
-13	BG to GG	80				8	8	6		15; F(20;35)
-14	GG with B-bands	30				6	8	6		F(10)
-15	GG with B-bands	30				11	11	9		30; F(5-20)
-16	BG	40			10	17	22	15		irreg; 40; F(15)
-17	BG with chlorite	50			10	23	28	11		5;60; F(15;20)
-18	BG with chlorite	50				22	25	2		25-60; F(15)
-19	BG with chlorite	80				11	11	3		30; 90; F(30)
-20	BG with chlorite	70			31	6	24	10		irreg; 10-60; F(crushed)
-21	GG with chlorite/BG	40			32	12	37	0		irreg; 30, 40, 80
-22	GG with chlorite/BG	40			15	13	23	10		30-50; F(30;40)
-23	GG with chlorite/BG	40			3	8	10	4		10-50; F(40)
-24	GG with chlorite	50				6	6	3		30-60; F(25;30)
-25	GG with chlorite	60				8	8	5		30; 45; F(10-25)
-26	BG with chlorite/GG	30				3	3	2		45; F(35)
-27	GG with B- and chl-bands	10			10	15	19	14		35-40; F(30)
-28	GG	25			5	13	15	12		40;80 F(30)
-29	GG	10				10	10	4		50; 60; F(10-25)
-30	GG with B-bands	30				4	4	3		20; F(40;45)
-31	GG	20				4	4	4		F(30)
-32	GG	20				6	6	2		25-45; F(30)
-33	GG/BG	60				6	6	6		F(25;35)
-34	GG with B-bands	40-50				6	6	6		F(25-40)
-35	GG	30				10	10	10		F(30;35)

Borehole KH-01-2012

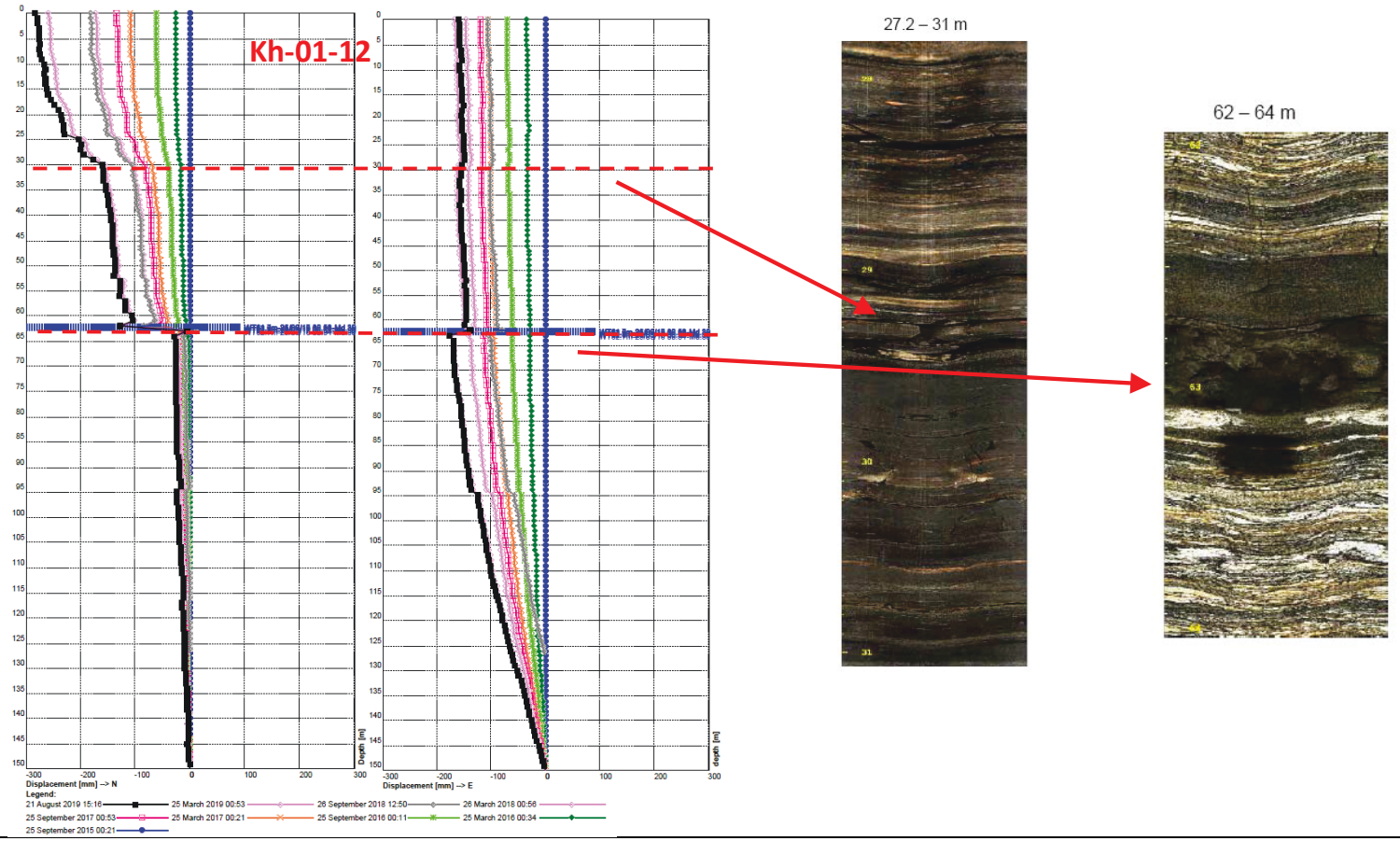

Borehole KH-01-2017

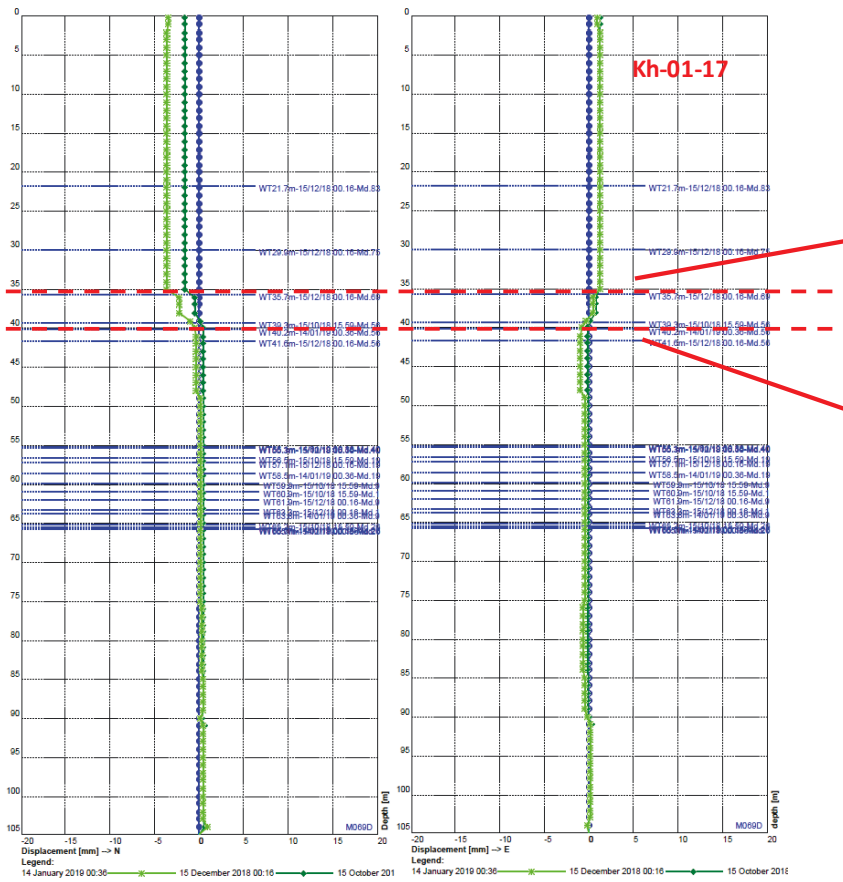

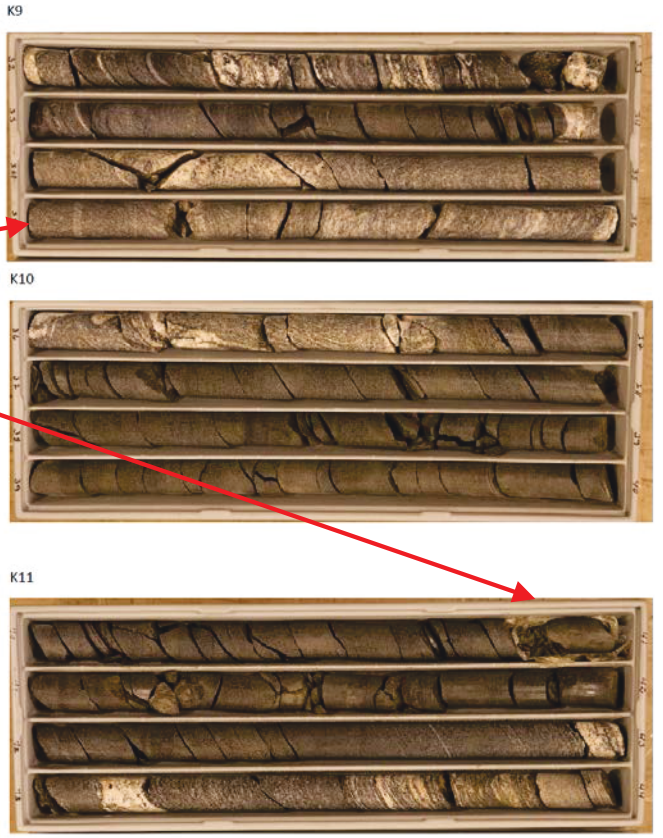

Borehole KH-02-2017

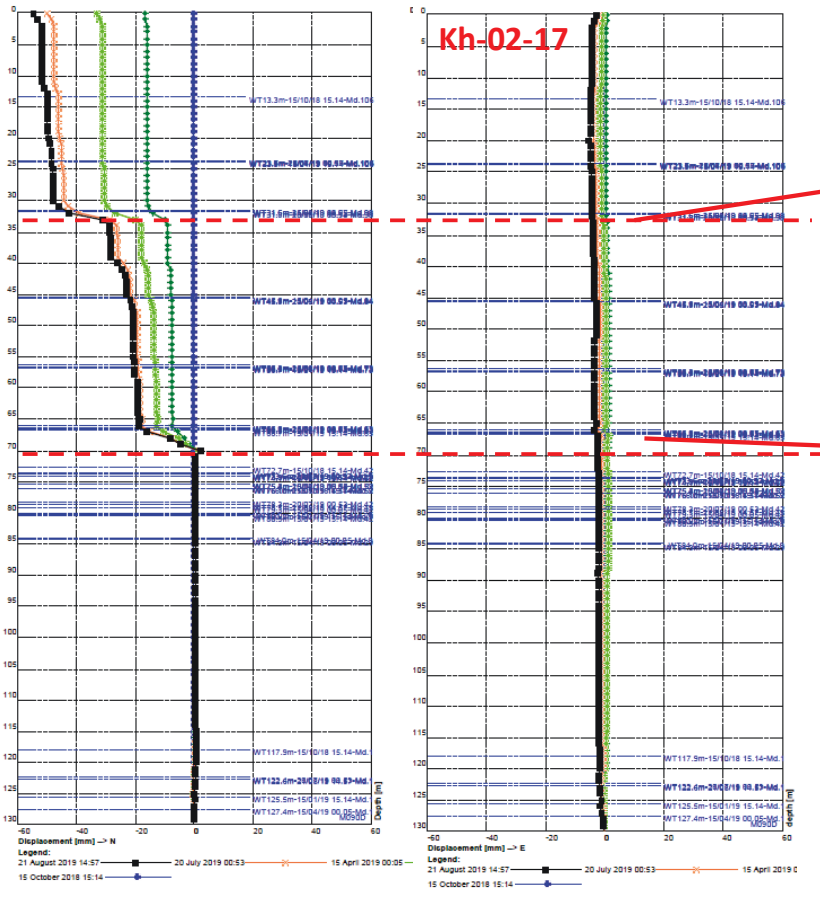

Borehole KH-01-2018

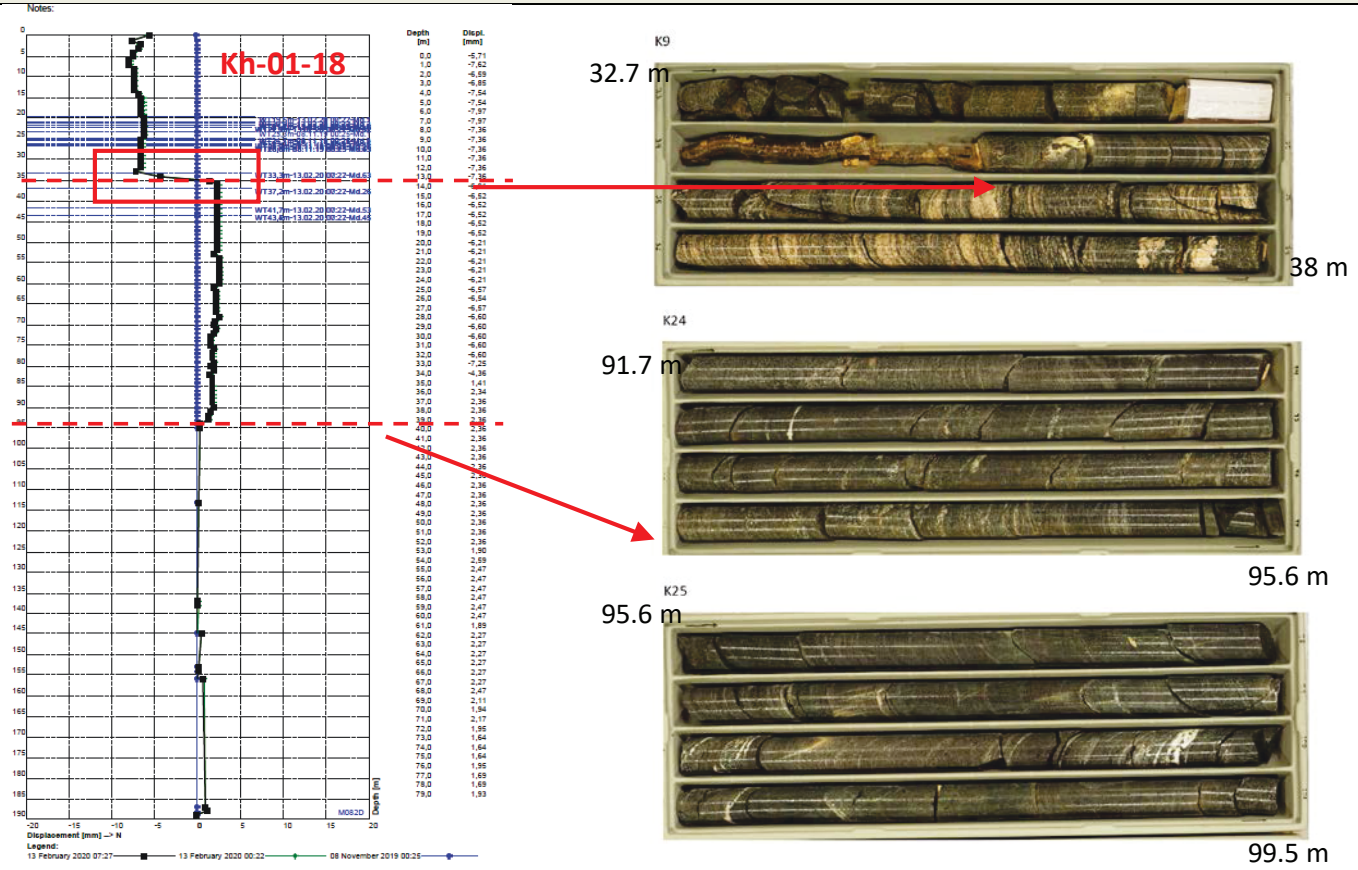

Borehole KH-02-2018

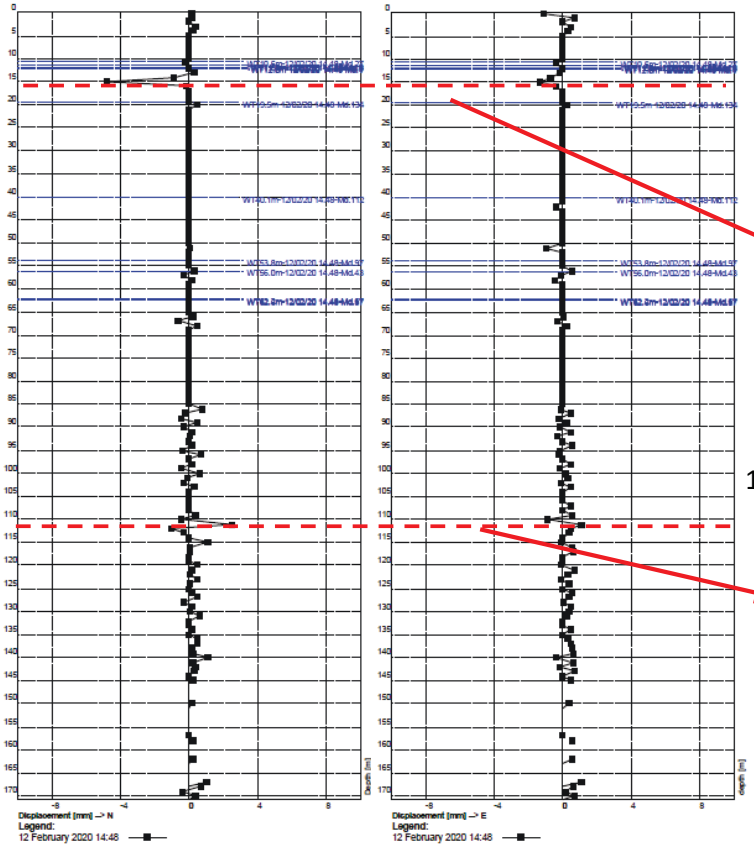

12 m

16 m

110.30 m

114.10 m

Appendix C

VELOCITY AND ACCELERATION FROM SELECTED DMS DATA:

Carried out on limited number of DMS data

DMS – KH-02-2017: Displacement at depths 20, 45, 75 and 100 m

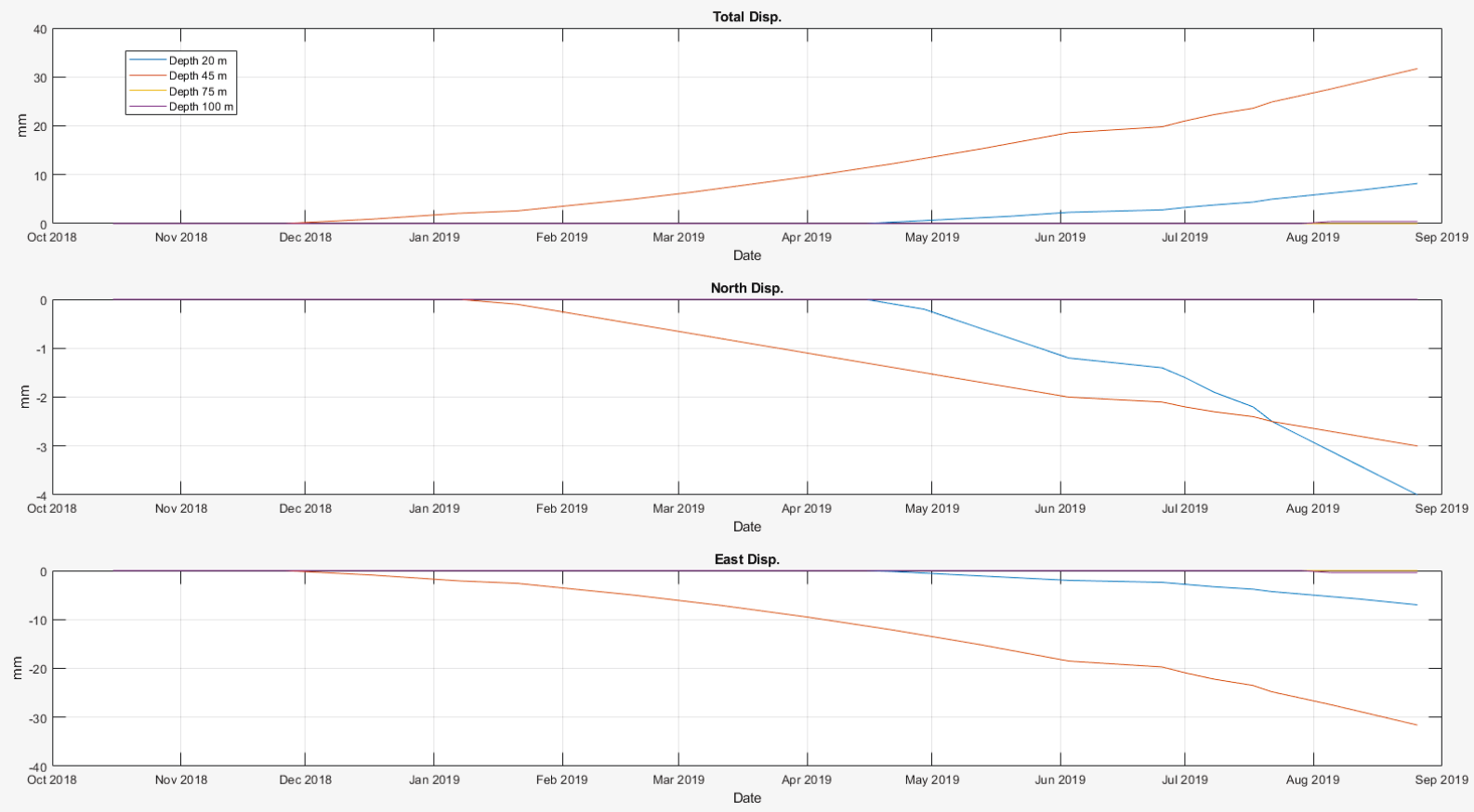

DMS – KH-02-2017: velocity and acceleration at depth 20 m

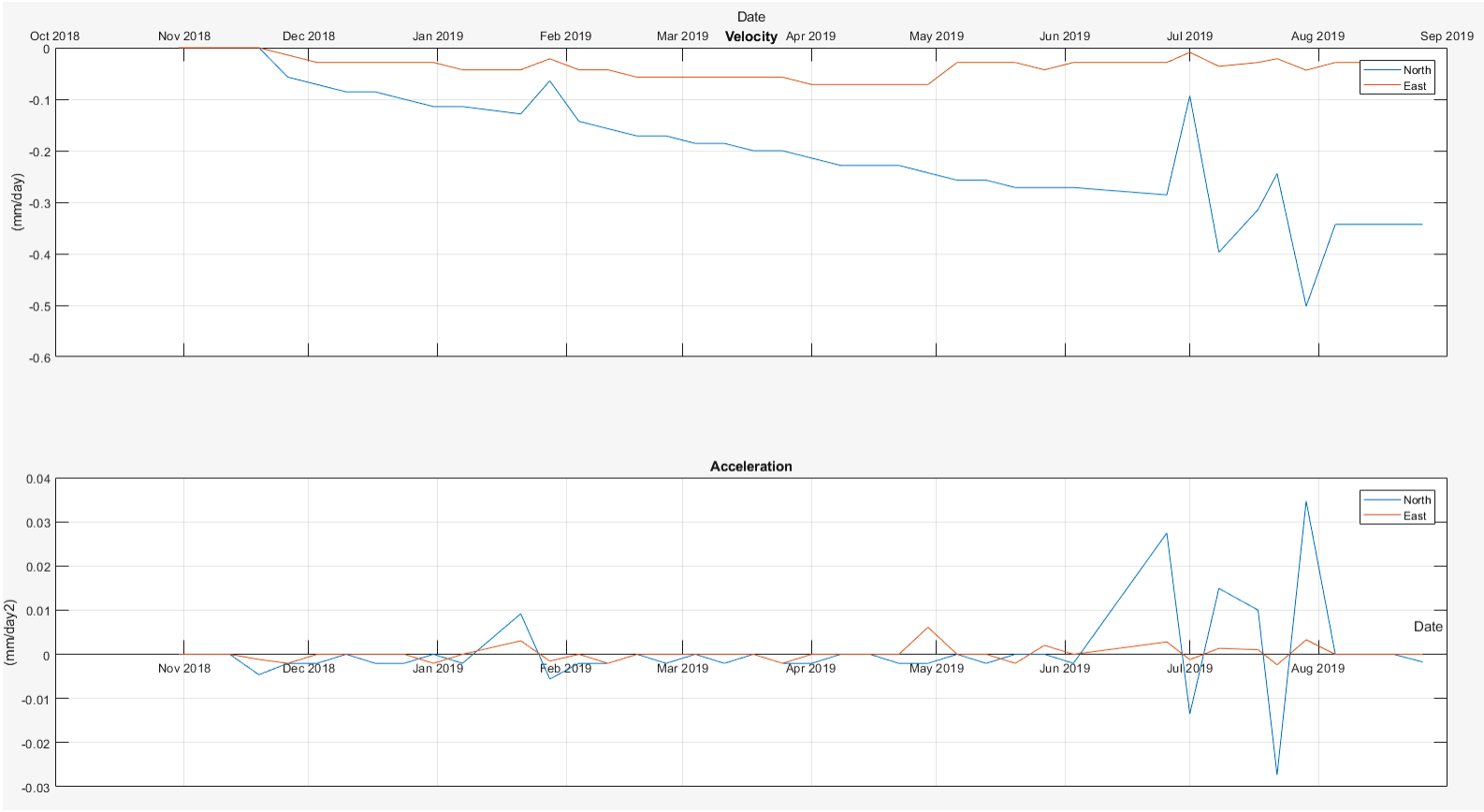

DMS – KH-02-2017: velocity and acceleration at depth 45 m

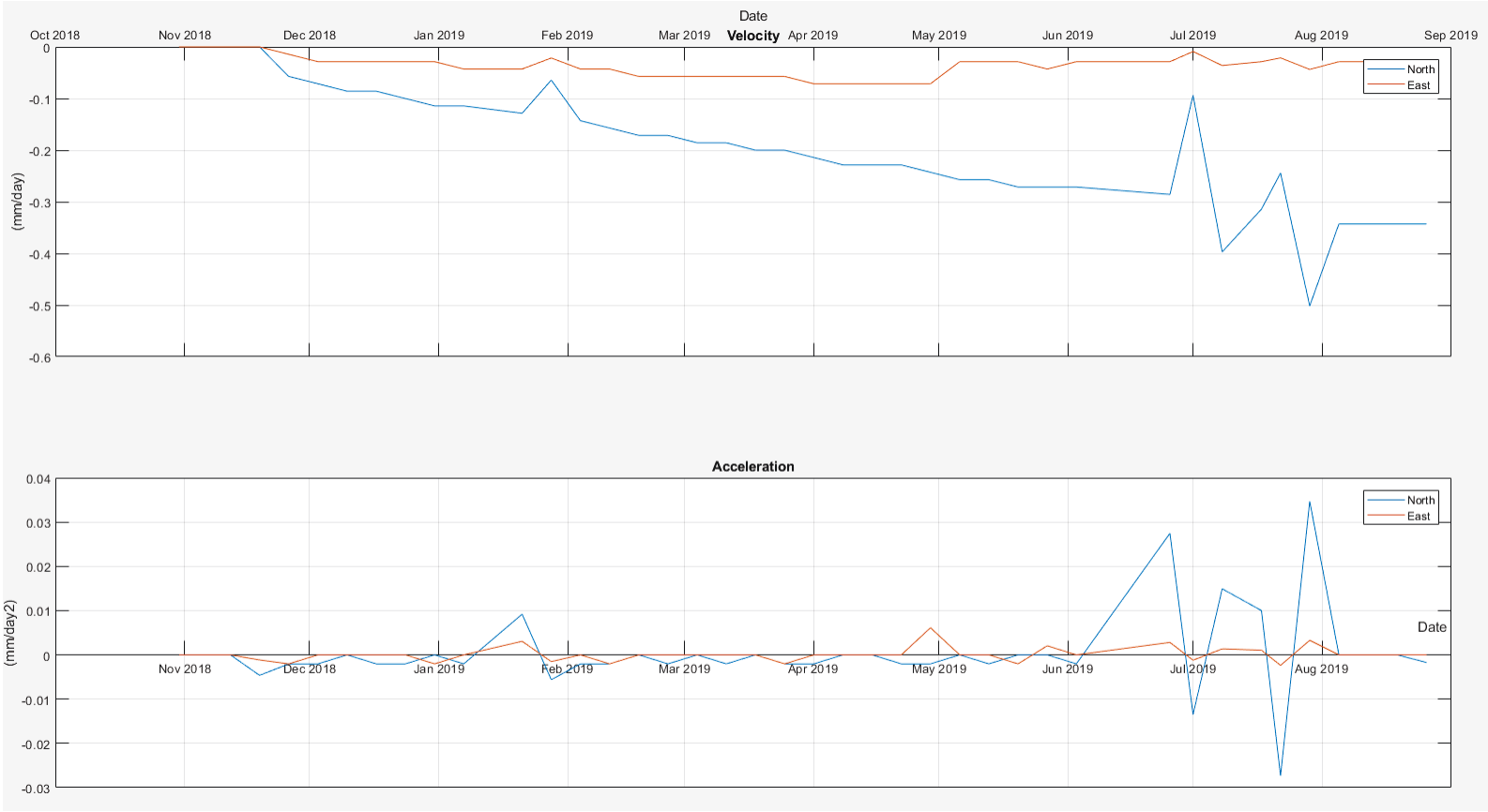

DMS – KH-01-2006: velocity and acceleration at depths 25, 35, 55, 80 m.

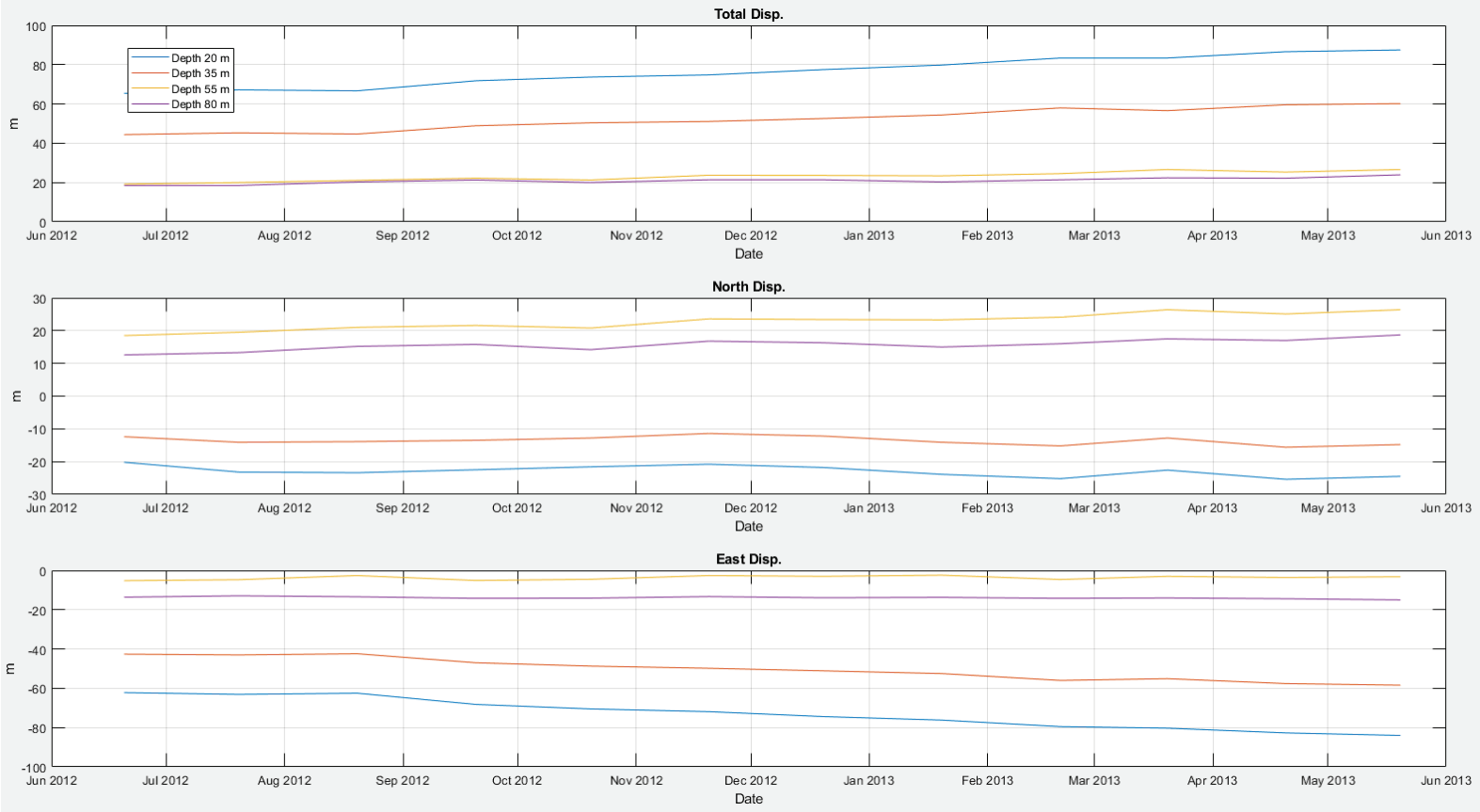

DMS – KH-01-2006: velocity and acceleration at depths 25 m.

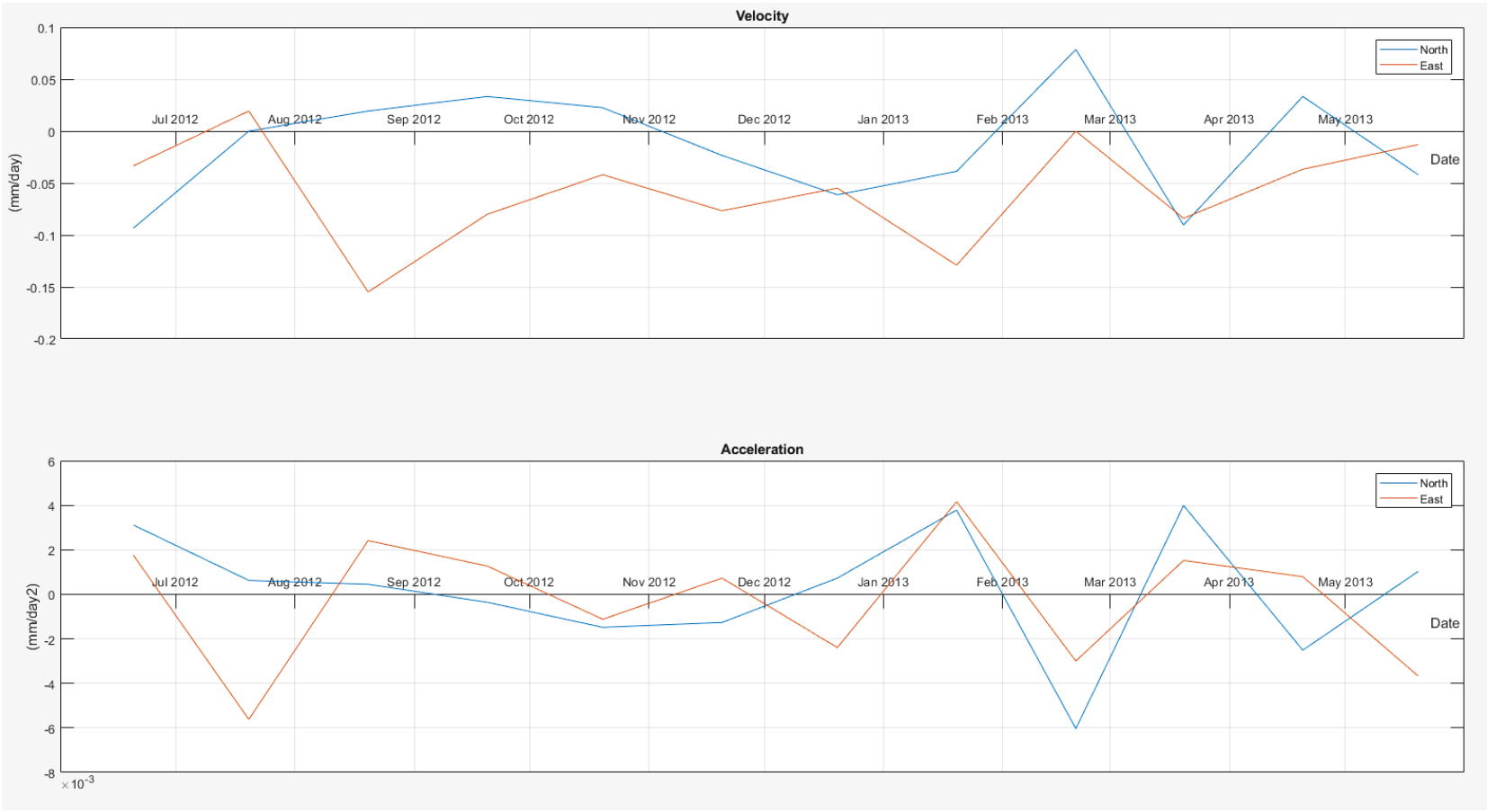

DMS – KH-01-2006: velocity and acceleration at depths 35 m.

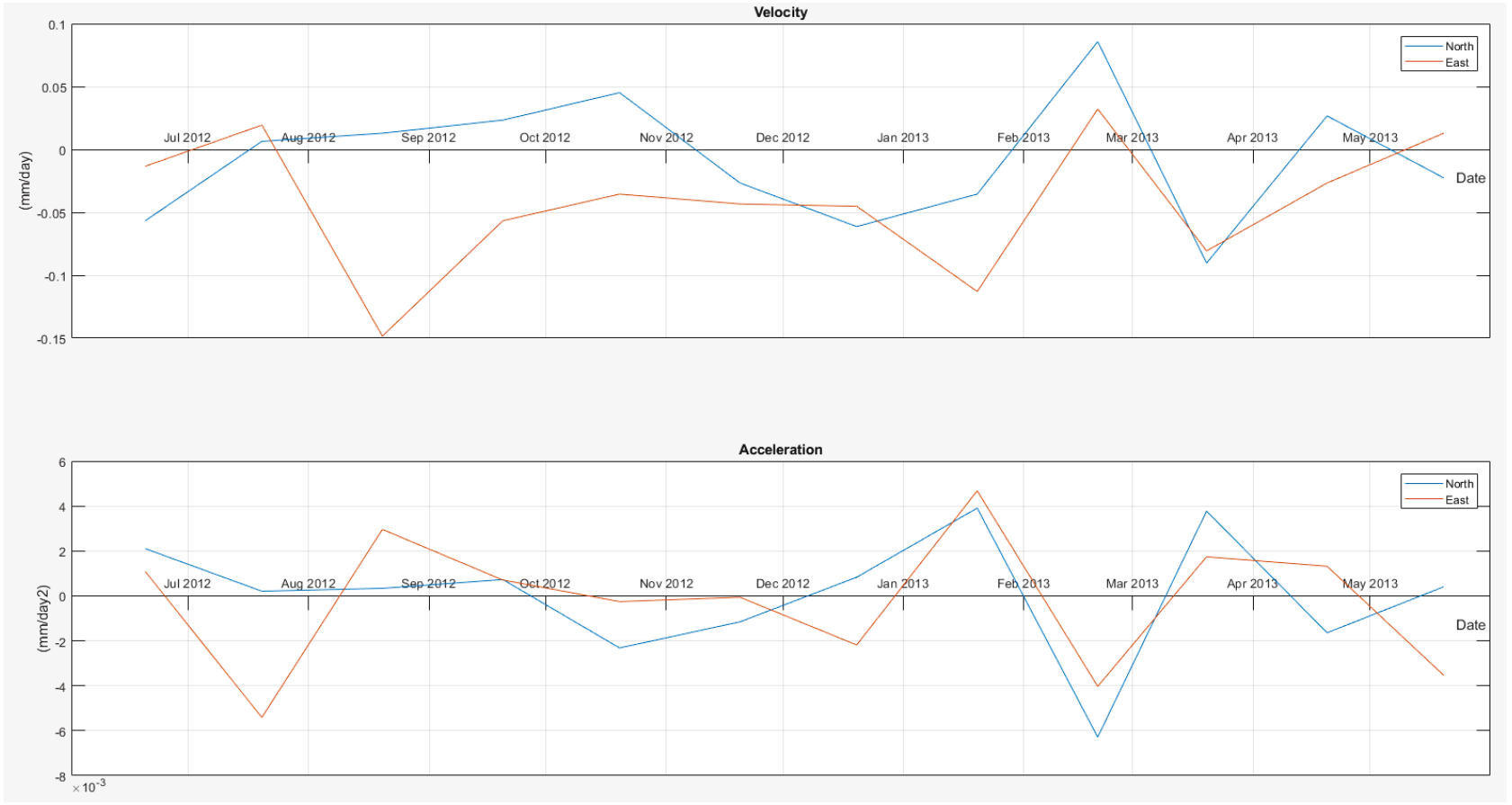

DMS – KH-03-2006: Displacement at depths 25, 45, 75, 100 m.

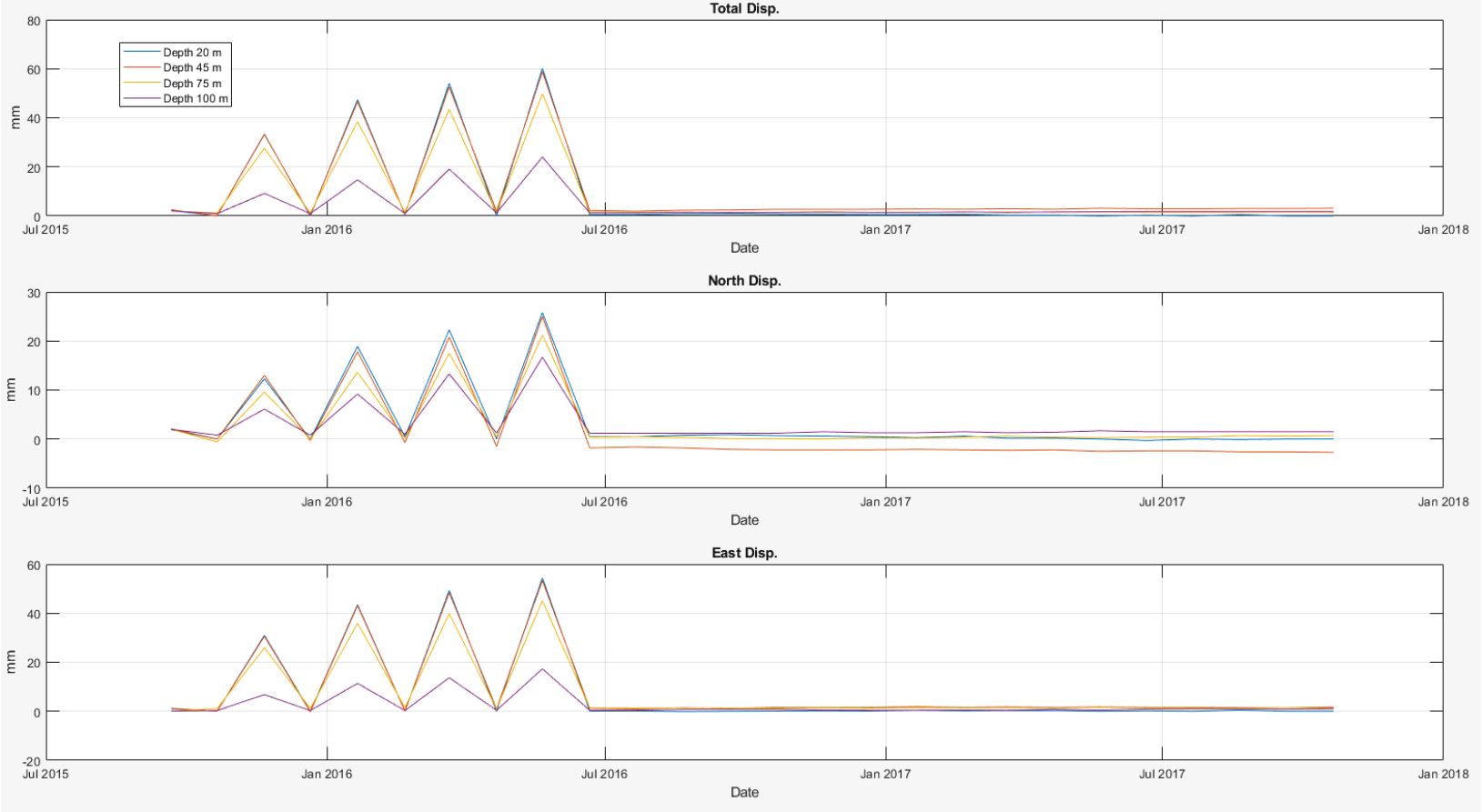

DMS – KH-03-2006: Velocity and acceleration at depths 25 m.

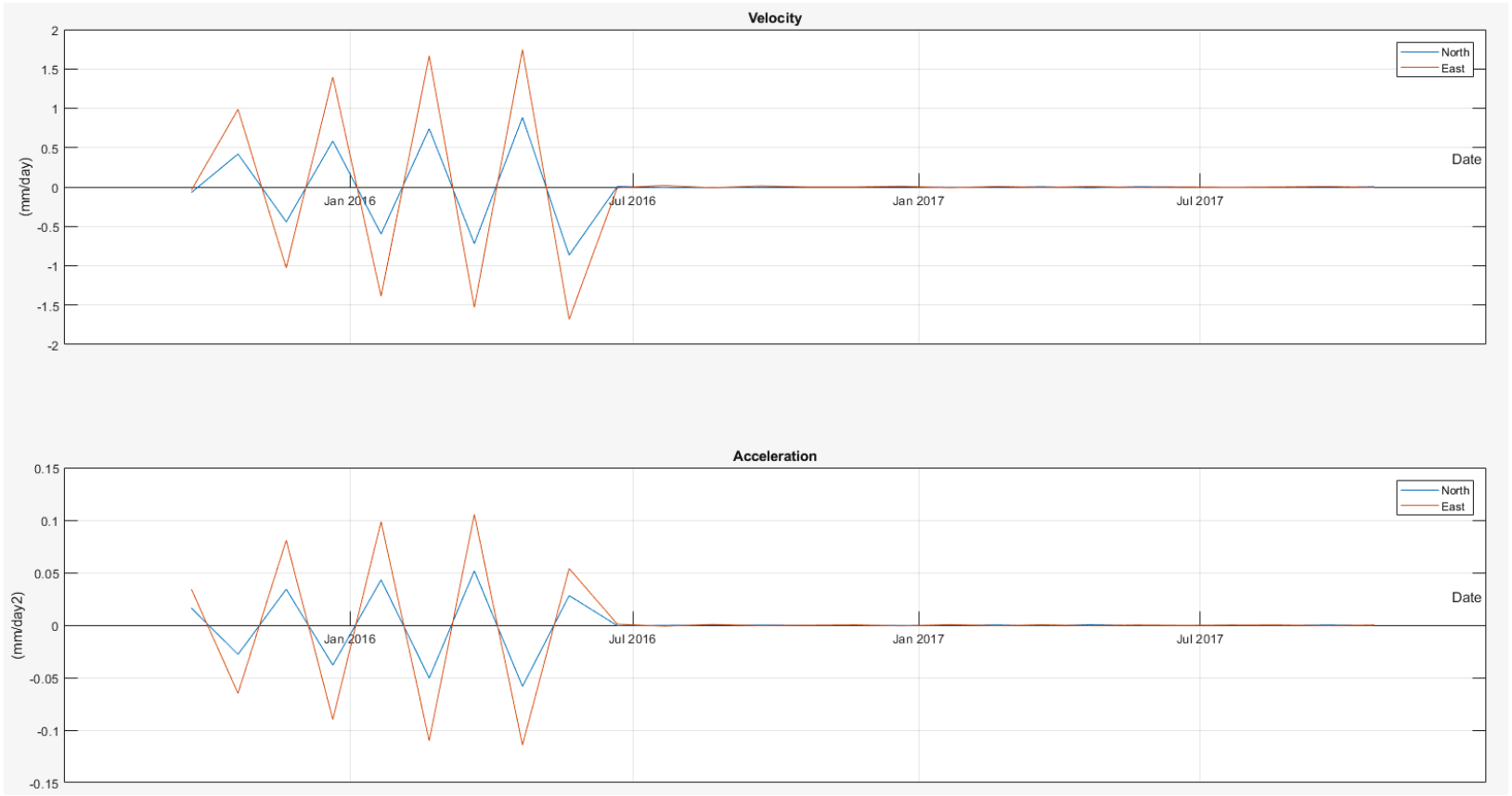

Appendix D

GEOLOGICAL CROSS-SECTIONS FOR
NUMERICAL MODELLING

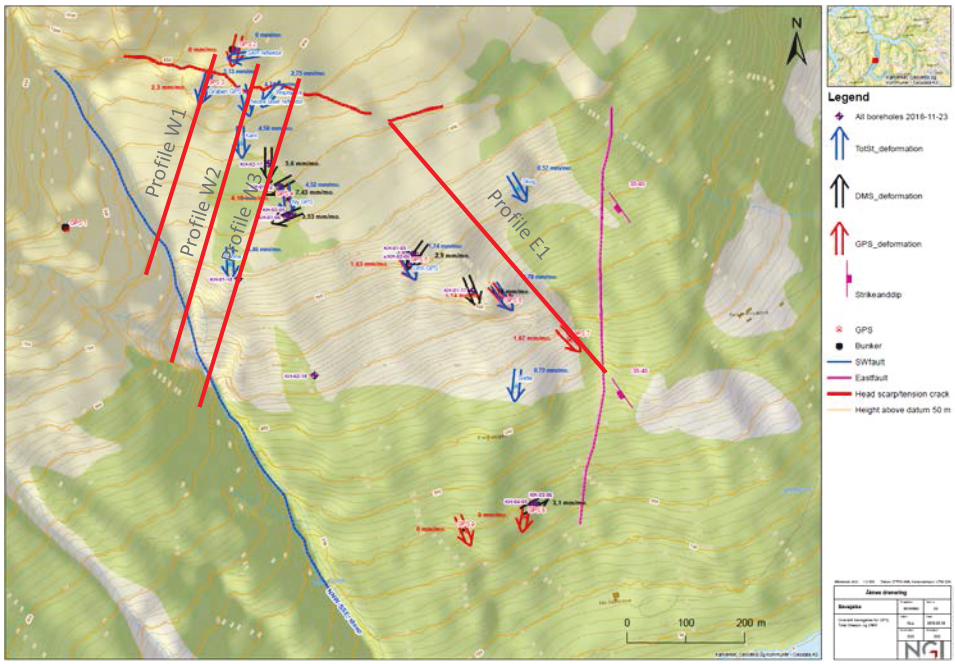
Profile W1
Profile W2
Profile W3
Profile E1
N
0
100
200 m
Legend
All boreholes 2016-11-23
TotSit_deformation
DMS_deformation
GPS_deformation
Strikeanddip
GPS
Bunker
SWfault
Eastfault
Head scarp/tension crack
Height above datum 50 m

Cross-section W1

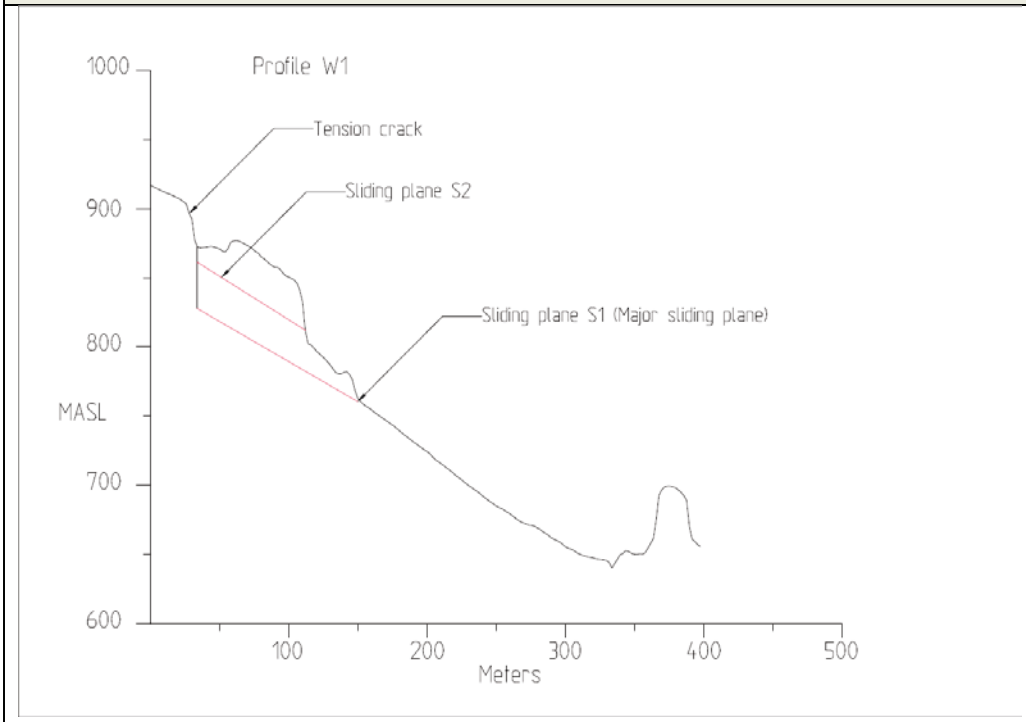

Cross-section W2

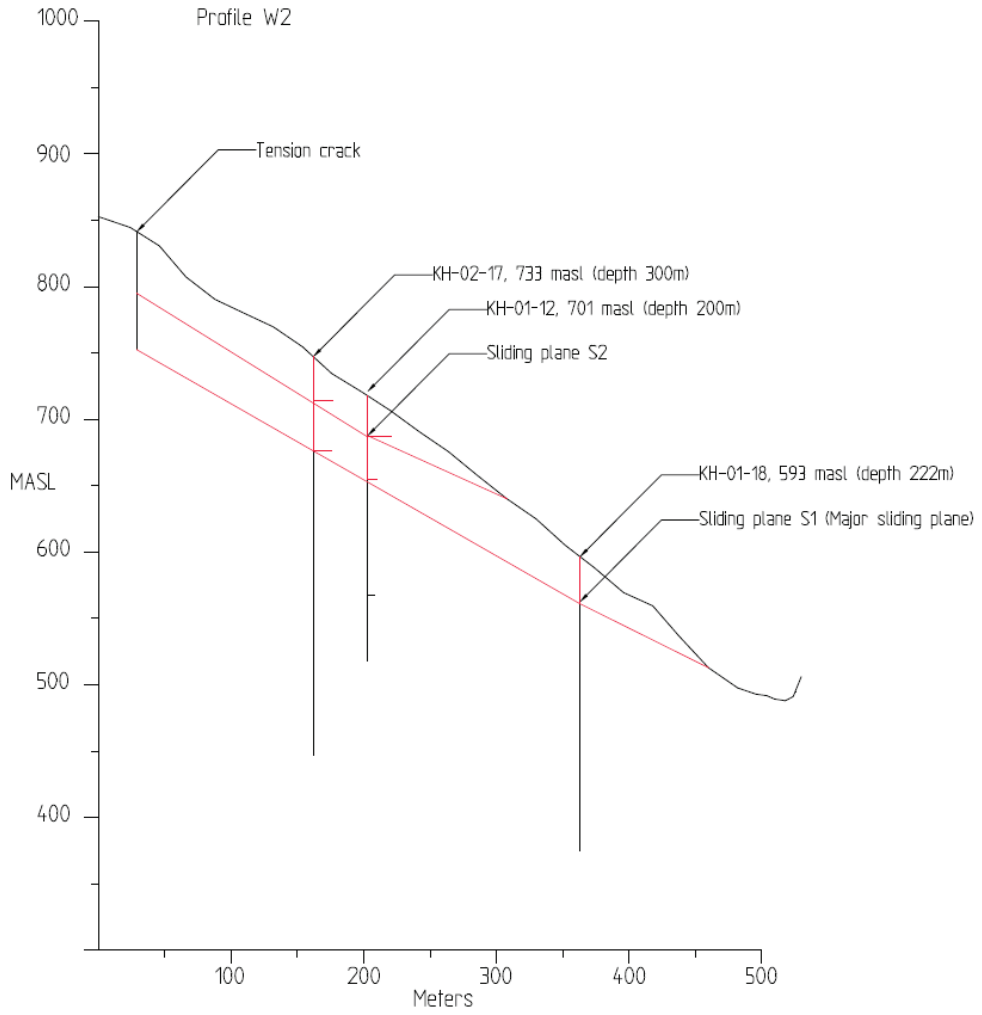

Cross-section W3

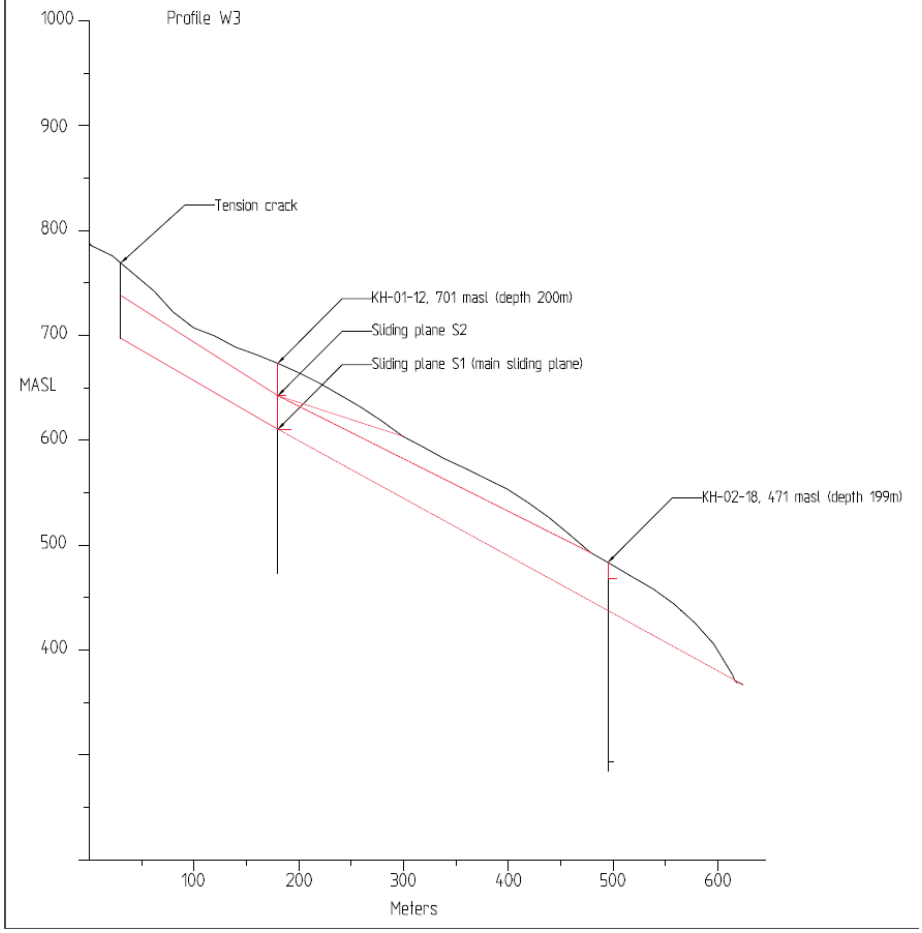

Cross-section E1

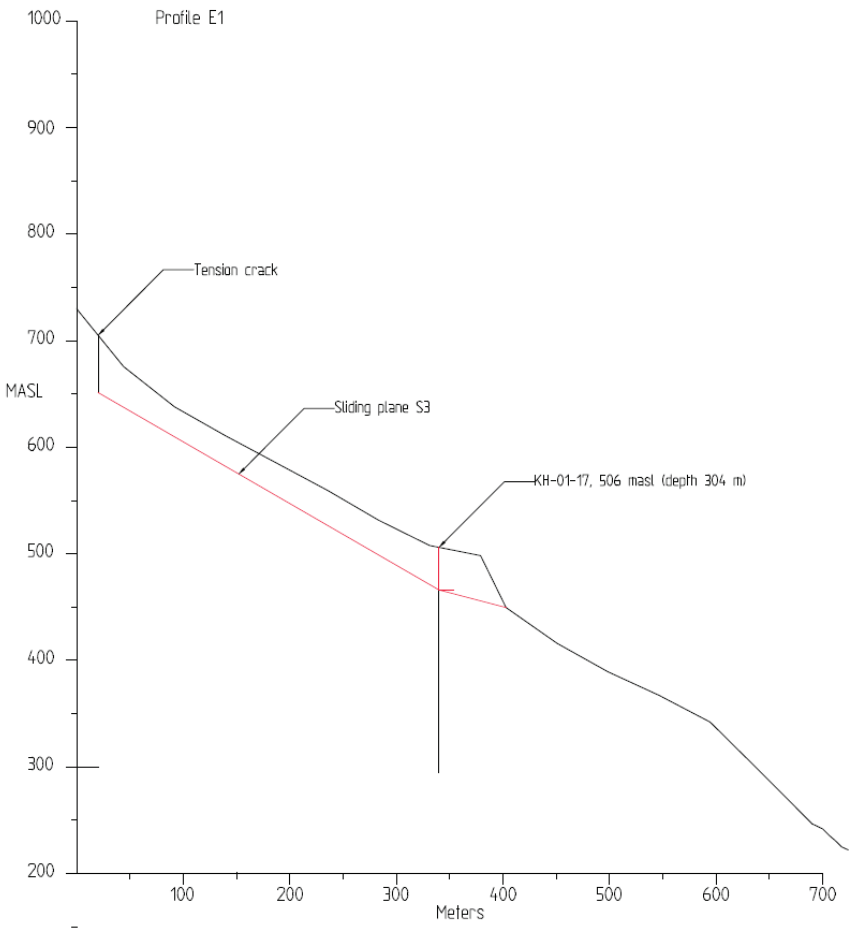

Kontroll- og referanseside/ Review and reference page

Dokumentinformasjon/*Document information*		
Dokumenttittel/*Document title* Åknes Rock slope - Monitoring of displacements		**Dokumentnr./*Document no.*** 20180662-05-R
Dokumenttype/*Type of document* Rapport / Report	**Oppdragsgiver/*Client*** NVE	**Dato/*Date*** 2020-07-09
Rettigheter til dokumentet iht kontrakt/ *Proprietary rights to the document according to contract* NGI		**Rev.nr.&dato/*Rev.no.&date*** 0 /
Distribusjon/*Distribution* BEGRENSET: Distribueres til oppdragsgiver og er tilgjengelig for NGIs ansatte / LIMITED: Distributed to client and available for NGI employees		
Emneord/*Keywords* Åknes, stability analysis, sliding plane, groundwater pressure		

Stedfesting/*Geographical information*	
Land, fylke/*Country* Norway	**Havområde/*Offshore area***
Kommune/*Municipality* Stranda	**Feltnavn/*Field name***
Sted/*Location* Åknes	**Sted/*Location***
Kartblad/*Map* 1219-2 Geiranger	**Felt, blokknr./*Field, Block No.***
UTM-koordinater/*UTM-coordinates* **Zone:** 33N**East:** 84568,29**North:** 6919727,39	**Koordinater/*Coordinates*** **Projection, datum: East: North:**

Dokumentkontroll/*Document control*
Kvalitetssikring i henhold til/*Quality assurance according to NS-EN ISO9001*

Rev/ *Rev.*	**Revisjonsgrunnlag/*Reason for revision***	**Egenkontroll av/ *Self review by:***	**Sidemanns-kontroll av/ *Colleague review by:***	**Uavhengig kontroll av/ *Independent review by:***	**Tverrfaglig kontroll av/ *Interdisciplinary review by:***
0	Original document	2020-06-29 Mahdi Shabanimashcool/ Kristin H. Holmøy	2020-07-07 Vidal Kveldsvik		

Dokument godkjent for utsendelse/ *Document approved for release*	**Dato/*Date***	**Prosjektleder/*Project Manager***
	9 July 2020	Kristin H. Holmøy

NGI (Norwegian Geotechnical Institute) is a leading international centre for research and consulting within the geosciences. NGI develops optimum solutions for society and offers expertise on the behaviour of soil, rock and snow and their interaction with the natural and built environment.

NGI works within the following sectors: Offshore energy – Building, Construction and Transportation – Natural Hazards – Environmental Engineering.

NGI is a private foundation with office and laboratories in Oslo, a branch office in Trondheim and daughter companies in Houston, Texas, USA and in Perth, Western Australia

NGI (Norges Geotekniske Institutt) er et internasjonalt ledende senter for forskning og rådgivning innen ingeniørrelaterte geofag. Vi tilbyr ekspertise om jord, berg og snø og deres påvirkning på miljøet, konstruksjoner og anlegg, og hvordan jord og berg kan benyttes som byggegrunn og byggemateriale.

Vi arbeider i følgende markeder: Offshore energi – Bygg, anlegg og samferdsel – Naturfare – Miljøteknologi.

NGI er en privat næringsdrivende stiftelse med kontor og laboratorier i Oslo, avdelingskontor i Trondheim og datterselskaper i Houston, Texas, USA og i Perth, Western Australia.

NGI
OSLO
TRONDHEIM
HOUSTON
PERTH

NORWEGIAN GEOTECHNICAL INSTITUTE
NGI.NO

Main office
PO Box 3930 Ullevaal St.
NO-0806 Oslo
Norway

Trondheim office
PO Box 5687 Torgarden
NO-7485 Trondheim
Norway

T (+47)22 02 30 00
F (+47)22 23 04 48
NGI@ngi.no

BIC NO. DNBANOKK
IBAN NO26 5096 0501 281
ORGANISATION NO.
958 254 318MVA

ISO 9001/14001
CERTIFIED BY BSI
FS 32989/EMS 612006